HISTONE VARIANT H2A.Z SUBSTITUTION MEDIATED BY THE SWR1-LIKE COMPLEX IS A NOVEL TRANSCRIPTIONAL REGULATORY MECHANISM CONTROLLING DEFENSE GENES AND IMMUNITY IN PLANTS

by

April Bonnard, B.S.

A thesis submitted to the Graduate Council of
Texas State University in partial fulfillment
of the requirements for the degree of
Master of Science
with a Major in Biology
August 2016

Committee Members:

Hong-Gu Kang, Chair

Nihal Dharmasiri

Sunethra Dharmasiri

FAIR USE AND AUTHOR'S PERMISSION STATEMENT

Fair Use

Duplication Permission

ACKNOWLEDGEMENTS

I would like to thank Dr. Hong-Gu Kang for his vast knowledge, expert guidance, and patience while advising me during my time in his lab. I have learned so much since the time I took his class as an undergraduate and have appreciated his unique teaching style, which pushed me to become a better student and researcher. I would also like to thank Yogendra Bordiya and Ji Chul Nam for their patience in training me, their assistance during my experiments, and their advice on experimental setup and troubleshooting. They have both encouraged me throughout the duration of my Master's degree and I would not have been able to accomplish the amount that I have without their help. I would also like to acknowledge Dr. Nihal Dharmasiri, Dr. Sunethra Dharmasiri, and all of the members in their lab for providing guidance during our weekly lab meetings. I must thank Dr. Ilha Lee and Dr. Daniel Zilberman for their generosity in supplying us with constructs and mutant plant lines. Additionally, I would like to thank the past and present undergraduates in our lab including Nicole Beisel, Jessica De La Torre, Rebecca Kilbourn, and Mario Aguilar for all of their help throughout this project. Lastly, I would like to thank my family, friends, and Jacob Rapp for supporting me through these two years of intense research.

TABLE OF CONTENTS

Page

LIST OF TABLES

LIST OF FIGURES

LIST OF ABBREVIATIONS

Abbreviation	Description
ACT1…….....	ACTIN 1, a component of the SWR1-like complex in Arabidopsis
ACT2…….	ACTIN2, a housekeeping gene
AH109……..	A yeast strain of mating type a (MATa)
ARP4……	ACTIN-RELATED PROTEIN 4, a component of the SWR1-like complex in Arabidopsis
AT…….	3-Amino-1,2,4-triazole, a chemical that acts as a competitive inhibitor of the product of the HIS3 gene.
ATP……..	Adenosine triphosphate, a high energy source for cells
CFU/ml…….	Colony forming units per milliliter
CHD…….	Chromodomain helicase DNA-binding family of chromatin-remodeling factors
Co-IP……	Co-immunoprecipitation, a molecular technique to identify protein-protein interactions *in vitro*
Col-0…….	Columbia ecotype of Arabidopsis thaliana
DNA…….	Deoxyribonucleic acid, the double helix containing anti-parallel strands of hereditary information constructed of nucleotides and a sugar-phosphate backbone
Dpi……	Days post infection

ETI……	Effector-triggered immunity, a robust immune response in plants that leads to HR
FLAG-tag……..….....	A protein tag with the sequence motif DYKDDDDK
FLS2…….	FLAGELLIN-SENSITIVE 2, a leucine-rich repeat transmembrane receptor kinase, one of many pattern-recognition-receptors (PRRs) responsible for the detection of bacterial flagellin (flg22)
Gal4 AD or BD…….	A transcription factor gene that produces either an activating domain or a binding domain protein required for the transcription of a reporter gene in a yeast two-hybrid screening
GFP……...	Green fluorescent protein, which emits green fluorescence when illuminated with light in the blue to ultraviolet range
GV2260……	A strain of *Agrobacterium tumefaciens*
H2A……..	A histone, two are found among the eight histones that together comprise a nucleosome
H2A.Z……...	One of many different variants of the histone H2A
His…….	The amino acid histidine
HIS3……..	A yeast two-hybrid reporter gene encoding imidazoleglycerol-phosphate dehydratase, the product of which encodes an enzyme required for the synthesis of histidine
HR…….	Hypersensitive response, a plant immune response initiated as a result of ETI to induce programmed cell death around the infection site

INO80……..	A family of chromatin-remodeling factors encompassing the INO80 and SWR1 complexes
ISWI…….	Imitation switch family of chromatin-remodeling factors
kDa……	Kilodalton, an atomic mass unit used here to describe the molecular weight of proteins
L40……	A yeast strain of the mating type a (MATa)
LexA BD or AD……..	A transcription factor gene that produces either an activating domain or a binding domain protein required for the transcription of a reporter gene in a yeast two=hybrid screening
luxCDABE……	A luminescent reporter gene cloned into the bacteria, *Pseudomonas syringae* pv. *tomato DC3000*
MIP……..	MORC1-interacting protein
MORC1……	MICROCHIDIA 1, also known as COMPROMISED RECOGNITION OF TURNIP CRINKLE VIRUS 1 (CRT1), required for optimum levels of plant immunity
mRNA……..	Messenger RNA, the product of gene transcription and the template for protein synthesis
Myc-tag……	A protein tag with the sequence motif EQKLISEEDL
NFR……..	Nucleosome-free region of the DNA
PAMP……..	Pathogen-associated molecular pattern
pB27…….	Bait plasmid for yeast two-hybrid screenings

PIE1……..	PHOTOPERIOD-INDEPENDENT EARLY FLOWERING 1, a component of the SWR1-like complex in Arabidopsis
pP6……	Prey plasmid for yeast two-hybrid screenings
PRR……..	Pattern recognition receptor
Pst…….	*Pseudomonas syringae* pv. *tomato DC3000*
PTI……	PAMP-triggered immunity
qRT PCR……..	Quantitative reverse transcription-polymerase chain reaction
R-proteins…….	Resistance proteins, which detect the presence of effector molecules emitted by pathogens
RdDM……...	RNA-directed DNA methylation
RIN1…….	RESISTANCE TO PSEUDOMONAS SYRINGAE PV MACULICOLA INTERACTOR 1, a component of the SWR1-like complex in Arabidopsis, also known as RVB1 and Tip49a
RNA…….	Ribonucleic acid, single stranded product of DNA transcription
RPM1……	RESISTANCE TO PSEUDOMONAS SYRINGAE PV MACULICOLA 1, R-protein
RPP5…….	RECOGNITION OF PERONOSPORA PARASITICA 5, R-protein
RVB1……	A component of the SWR1-like complex in Arabidopsis, also known as RIN1 and Tip49a
SAIL……..	Syngenta Arabidopsis Insertion Library, a naming system for mutant seeds produced

SALK……	A seed-naming system for seeds produced at the Salk Institute
SDS-PAGE……...	Sodium dodecyl sulfate-polyacrylamide gel electrophoresis, a method for separating proteins by size
SEF……...	SERRATED LEAVES AND EARLY FLOWERING, also known as SWC6, a component of the SWR1-like complex in Arabidopsis
SUF3…….	SUPPRESSOR OF FRI 3, also known as ARP6, a component of the SWR1-like complex in Arabidopsis
SWC2……...	A component of the SWR1-like complex in Arabidopsis
SWC5……...	A component of the SWR1-like complex in Arabidopsis
SWC6……...	A component of the SWR1-like complex in Arabidopsis, also known as SEF
SWI/SNF……..	Switch/Sucrose Non-Fermentable, a family of chromatin-remodeling factors
SWR1 complex…….	A chromatin-remodeling factor in yeast responsible for the replacement of H2A.Z for H2A
T-DNA……..	Transfer DNA, transferred from bacteria to a host with the purpose of rendering a host protein nonfunctional
TAIR…….	The Arabidopsis Information Resource, a database of genetic and molecular biology data for *Arabidopsis thaliana*

Tip41…….	Tap42-interacting protein of 41 kDa, a housekeeping gene
Tip49a……...	TATA Binding Protein Interacting Protein 49 KDa, a component of the SWR1-like complex in Arabidopsis, also known as RIN1 and RVB1
UBC……..	Ubiquitin-conjugating enzyme, a housekeeping gene
UTR……..	Untranslated region of DNA
WRKY……..	A transcription factor that regulates transcriptional reprogramming in response to plant stress responses
WT……	Wild-type ecotype, in this sense it refers to Col-0
Y187…….	A yeast strain of the mating type α (MATα)
Y2H……...	Yeast two-hybrid, a technique used to identify protein-protein interactions *in vivo*
YAF9……	A component of the SWR1-like complex in Arabidopsis

ABSTRACT

Plants have evolved a complex immune system as a result of an evolutionary arms race between the host and various pathogens. One of the most vigorous immune responses in plants involves resistance (R) proteins, which detect the presence of effector molecules from pathogens and trigger a large-scale reprogramming in RNA transcription of defense genes. MORC1 is one of few proteins that have been shown to interact with several of these R-proteins and is required for optimum immune responses in Arabidopsis against a wide range of pathogens. MORC1 has been speculated to be involved in remodeling chromatin in response to pathogen infection as it has been shown to exhibit ATPase and endonuclease activity and its nuclear population increases after pathogen infection. Through a co-immunoprecipitation, we found that MORC1 physically interacts with several chromatin-remodeling factors including ACT1, ARP4, SWC2, SWC6, SUF3, PIE1, RVB1, and YAF9. These factors belong to the SWR1-like complex in Arabidopsis whose yeast homolog functions to exchange the histone H2A for its variant, H2A.Z. This replacement has been speculated to be involved in transcription regulation as it occurs in the promoter and/or genic region of actively transcribed genes. Interestingly, mutations in a few SWR1-like components led to altered resistance to the bacterial pathogen *P. syringae*, suggesting that the SWR1-like complex functions in plant immunity. In fact, a previous study revealed that RVB1, also known as Resistance to *Pseudomonas syringae* pv *maculicola* Interactor 1 (RIN1), interacts with the R-proteins, RPM1 and RPP5, and has been shown to be a negative regulator of plant defense

responses. Interestingly, RVB1 and MORC1 interacted in both the nucleus and microsomes. To further gain insight into the molecular mechanism of this H2A.Z replacement in defense signaling, I performed chromatin immunoprecipitation with H2A.Z and found that infection with *P. syringae* leads to an elevated level of chromatin associated with H2A.Z including defense genes such as *PR-5*. Furthermore, an Arabidopsis mutant line lacking three genes encoding *H2A.Z* showed altered transcriptional induction of defense genes in response to pathogen infection. Together, these results establish that the histone replacement with H2A.Z by the SWR1-like complex modulates the transcription of defense genes and thereby likely affects immunity in plants.

CHAPTER I

Introduction: chromatin-remodeling and its association with immunity in plants

Plants have been evolutionarily competing with infectious pathogens for millions of years, the effect of which continuously advanced the complexity of their immune system. These infectious pathogens contain pathogen-associated molecular patterns (PAMPs), such as flagellin in bacteria. This PAMP is then detected in the plant by pattern recognition receptors (PRRs), such as FLS2, which is located on the plasma membrane [1-5]. This detection initiates downstream signaling in plant cells, which leads to altered chromatin accessibility in the nucleus in order to regulate the transcription of genes for a proper immune response [3, 6]. This level of defense is known as PAMP-triggered immunity (PTI) [7, 8]. It is possible, however, for such pathogens to secrete effector molecules or virulence factors into the host cell to repress the host immune responses [7, 9-11]. To combat this repression, the plant resistance (R) proteins can detect some of these effectors, which will then elicit an even more robust immune response than from PTI alone, and is commonly referred to as effector-triggered immunity (ETI) [1, 7, 12]. This then mostly leads to the hypersensitive response (HR), in which apoptosis (cell death) occurs around the area of infection in order to diminish the nutrient supply to the pathogen and restrict its mobility, preventing further infection to other tissues of the plant [7, 13].

MORC1 is a protein that interacts with several R proteins [13] and is required to maintain optimum levels of immunity in Arabidopsis [13-15]. It has been shown that MORC1 resides in endosome-like vesicles in the cytoplasm and that, upon infection of

the plant with *Pseudomonas syringae* pv. *tomato DC3000* (*Pst*), the nuclear concentration of MORC1 increases [14, 15]. This suggests that MORC1 may shuttle to the nucleus in order to regulate the transcription of genes required for proper immune responses. MORC1 has been shown to be an ATPase as well as an endonuclease [13, 14], whose activities are frequently associated with a chromatin-remodeling factor. In the nucleus, it has been shown that MORC1 is predominantly associated with heterochromatin, and plays a role in heterochromatin condensation [14, 16]. MORC1 and one of its six homologues, MORC6, have also been shown to be involved in the RNA-directed DNA methylation (RdDM) pathway, which functions, along with other proteins such as chromatin-remodeling factors, in the methylation of DNA [17]. This methylation is associated with gene silencing, more specifically as a secondary mechanism to stabilize genes that have already been silenced [18], although the direct involvement of MORC1 in RdDM is currently debatable.

Adequate cellular responses depend on chromatin-remodeling factors, which modify chromatin by either moving, ejecting, or restructuring nucleosomes. Nucleosomes consist of 147 base pairs of DNA wrapped around 8 core canonical histones: H2A, H2B, H3, and H4 [19]. Chromatin-remodeling becomes particularly pronounced when cells are under stress [20], raising a possibility that chromatin-remodeling factors are important players in biotic stress responses. Chromatin-remodeling factors are classified into four families – SWI/SNF, ISWI, CHD, and INO80, based on common structural and functional aspects of the complexes [19]. The SWI/SNF-Related complex (SWR1 complex) in yeast is a chromatin-remodeling factor, which belongs to the SWI/SNF family [21, 22]. It is involved in histone replacement – specifically the exchange of the

H2A-H2B canonical dimer for that of H2A.Z-H2B in a replication-independent manner [19, 22, 23]. This histone exchange occurs predominantly on nucleosomes flanking an unstable nucleosome-free region (NFR), such that the gene can become stably accessible for transcription [24, 25]. This histone exchange mark is actually the predominant form of active eukaryotic genes [26]. It ultimately promotes gene expression and several lines of evidence reveal that H2A.Z deposition is indeed inversely related to DNA methylation [27, 28] and that the two are mutually antagonistic [29]. Thus, these observations raise a possibility that the activity of the SWR1-like complex may be antagonistic to that of MORC1.

The H2A.Z exchange is required for proper cell development as it functions not only to activate genes, but also to retain transcriptional memory, regulate thermal sensory responses, aid in the progression of the cell cycle, and prevent heterochromatic regions of the DNA from spreading to euchromatic areas [21, 30, 31]. In yeast, H2A.Z regulates gene responsiveness in relation to environmental changes [30]. For example, it is required for proper regulation of oleate-responsive genes as well as phosphate starvation and thermosensory response genes [25, 32, 33]. It has been shown that the INO80 complex is responsible for creating the NFR to which the flanking nucleosomes become modified through histone exchange by the SWR1 complex [34]. In addition, the INO80 complex functions as a regulatory component for the SWR1 complex in that it replaces misplaced H2A.Z histone variants for the original H2A histones [35].

The SWR1 complex in yeast is comprised of 14 proteins [36] as shown in Figure 1, whereas its counterpart in Arabidopsis is not as well characterized. To date, at least 11 putative homologues that belong to the SWR1 complex may be found in Arabidopsis

based on protein interaction studies and *in silico* analysis [27] as shown in Table 1, which also includes homologues from Drosophila and human. Many components of the SWR1-like complex are associated with plant immunity. In a study by March Díaz et al., it was found that ARP6 (SUF3), SEF (SWC6), and PIE1 are all required for ideal levels of immunity in Arabidopsis [23]. When they tested the expression of *pathogenesis-related 1* (*PR-1)* as well as a variety of genes involved in the SAR (systemic acquired resistance) response, most defense genes tested were constitutively expressed in both *swc6* and *pie1* plants [23]. In addition, the knock-down mutant *rvb1* showed increased R-dependent responses, indicating that the protein RVB1 acts as a negative regulator of R-dependent responses and thus plant immunity [37, 38]. While multiple members in the SWR1 complex have known immunity-associated functions, the underlying molecular mechanism how chromatin-remodeling affects immunity in plants is unclear, which strongly justified my study to further characterize the SWR1 complex in conjunction with MORC1.

One of best characterized SWR1-like complex components in plants, RVB1, also known as RIN1, Tip49a, RuvBL1, Tip48/Tip49, ECP-54, Pontin, Tih1, p50, and Tap54β [39], is a member of the AAA+ ATPase family of proteins [27, 36]. RVB1 has been shown to interact with the R-proteins RPM1 (Resistance to *Pseudomonas syringae* pv. *maculicola 1)* and RPP5 (Recognition of *Peronospora parasitica 5)* in Arabidopsis [38], and has been shown to be a negative regulator of *R* gene-dependent immunity in that the hemizygous mutant significantly reduces the amount of hyphal growth in the leaves of the plant as compared to the wild type (WT) and that the expression of *PR-1* is significantly elevated in the mutant [38]. In the nucleus, RVB1 forms a heterohexamer

with RVB2 and assembles onto the SWR1-like complex [36]. It associates with a wide range of proteins including the RNA polymerase II holoenzyme, telomerase complex, microtubules during cell division and Rab5 in endosomes to support Ras-mediated endocytosis [40-44]. All of these functions are necessary for proper growth and development and support the fact that RVB1 is an essential protein since its loss of function mutation leads to lethality [27, 45]. Because RVB1 plays a role in both epigenetics as well as plant immunity, I further focused on this SWR1-like complex component in conjunction with MORC1 to gain insight into the relationship between chromatin-remodeling and immunity in plants.

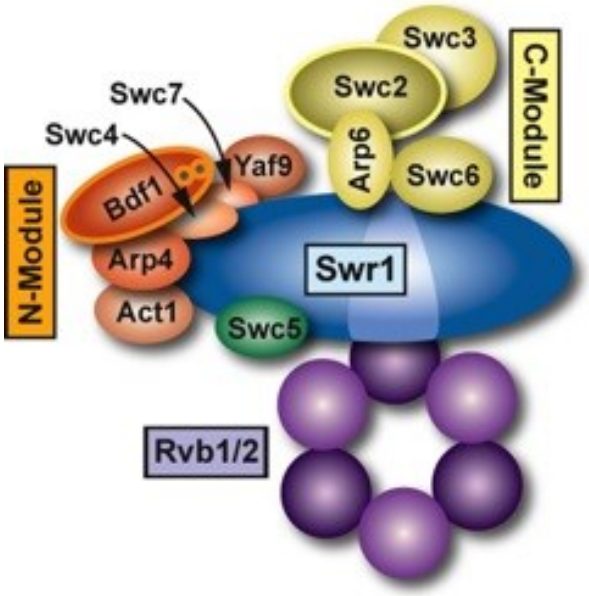

Figure 1. The 14 components of the SWR1 complex in yeast.
Note that this figure is adapted from [36]**.** No changes were made to this image and it was used under the Creative Commons license found here: http://creativecommons.org/licenses/by/3.0/legalcode

Table 1. Components of the yeast SWR1 complex and their homologues in humans and Arabidopsis. Note that this table is modified from [27].

S. cerevisiae SWR1 complex	*H. sapiens* SRCAP complex	*A. thaliana* SWR1-like complex	Locus
Swr1	SRCAP	PIE1	At3g12810
Arp4	BAF53a	ARP4	At1g18450
Arp6	ARP6	ARP6/SUF3/ESD1	At3g33520
Yaf9	GAS41	TAF14	At2g18000
-	-	TAF14b	At5g45600
Rvb1	TIP49a	TIP49a/RIN1	At5g22330
Rvb2	TIP49b	RVB2A	At5g67630
-	-	RVB2B	At3g49830
Swc2	YL1	SWC2	At2g36740
Swc3	-	-	-
Swc4	DMAP1	SWC4	At2g47210
Swc5	-	SWC5	At5g30490
Swc6	ZnF-HIT1	SEF	At5g37055
Swc7	-	-	-
Act1	Actin	ACT1	At2g37620
-	-	ACT2	At3g18780
-	-	ACT3	At3g53750
-	-	ACT4	At5g59370
-	-	ACT7	At5g09810
-	-	ACT8	At1g49240
-	-	ACT11	At3g12110
-	-	ACT12	At3g46520
Htz1	H2A.Z	HTA8	At2g38810
-	-	HTA9	At1g52740
-	-	HTA11	At3g54560

CHAPTER II

Physical association of MORC1 with SWR1-like chromatin-remodeling complex

MORC1 is physically associated with multiple components of the SWR1-like chromatin-remodeling complex *in planta*

In order to determine if chromatin-remodeling factors comprising the SWR1-like complex interact with MORC1 *in planta*, a co-immunoprecipitation (Co-IP) was performed using nine of the protein components. To this end, estradiol-inducible vectors [46] carrying FLAG-tagged chromatin-remodeling factors and Myc-tagged MORC1 were constructed and transformed into the Agrobacteria strain GV2260, which were subsequently infiltrated into *Nicotiana benthamiana*. Proteins were then extracted from the tissue 2 days after spraying with 30μM estradiol, which induces the transgenes, and subjected to Co-IP experiments. Anti-FLAG antibody conjugated agarose beads were used to immunoprecipitate FLAG-tagged proteins and association of Myc-tagged proteins was analyzed.

The Co-IP result revealed that a majority of SWR1-like complex proteins display physical interactions with MORC1, including ACT1, ARP4, SWC2, SWC6, SUF3, PIE1, RVB1, and YAF9 (Figure 2). The two bands corresponding to MORC1 are indicative of the original (the higher band in the top panel in the Figure 2) as well as the post-translationally modified form (the lower band in the top panel in the Figure 2) of the protein [15]. It is not surprising that MORC1 displayed interaction with RVB1, as both proteins interact with the R-protein RPM1, which is located on the plasma membrane [15, 38, 47]. It was interesting nonetheless that 8 of the 9 chromatin-remodeling factors

interacted with MORC1, all except SWC5. These results suggest that MORC1 may interact in the nucleus with the components of the SWR1-like complex, which function to remodel chromatin in response to pathogen infection.

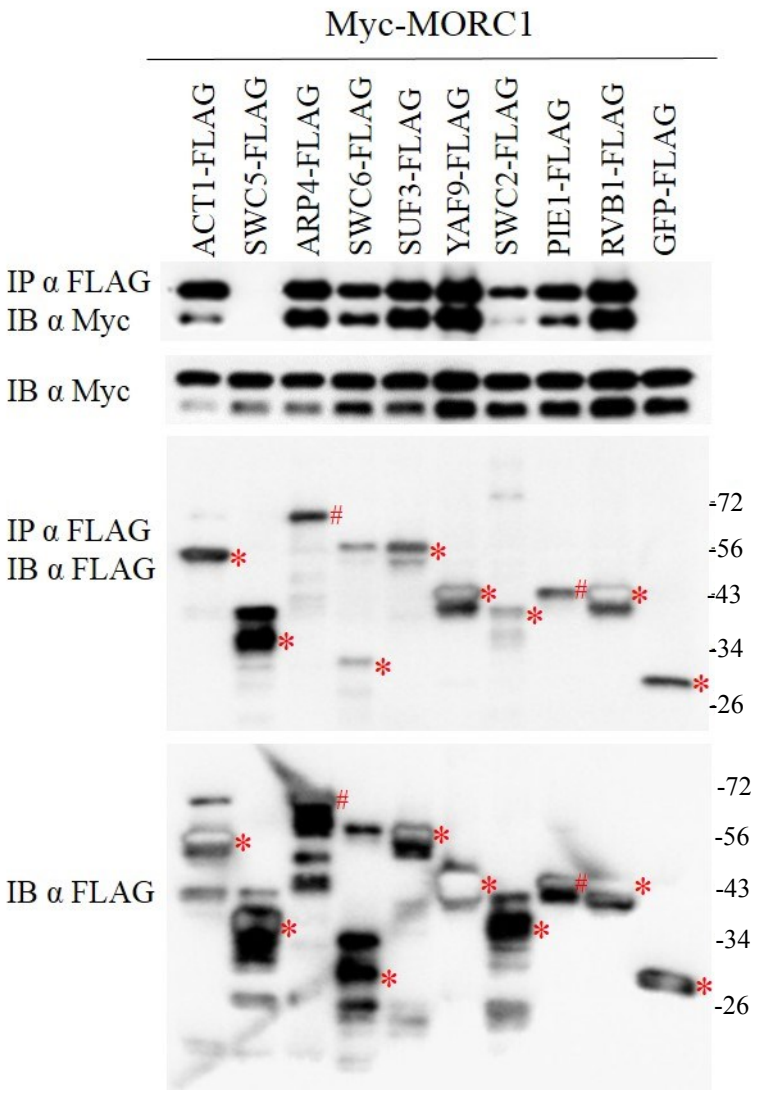

Figure 2. Co-immunoprecipitation (Co-IP) reveals that MORC1 interacts with several components of the SWR1-like complex. Results indicate that of all proteins tested, those that display interaction with MORC1 include: ACT1, ARP4, SWC2, SWC6, SUF3, PIE1, RVB1, and YAF9. A FLAG-tagged GFP was used as a negative control. (* indicates that the expected protein sizes are within 10 kDa of what is shown, and # indicates that the expected protein sizes are outside of 10 kDa of what is shown.)

Yeast two-hybrid assay failed to show the interaction of MORC1 with SWR1-like complex proteins

A yeast two-hybrid (Y2H) assay was performed in order to further confirm physical interactions between the chromatin-remodeling factors and MORC1 as shown in Figure 2. All nine chromatin-remodeling factors tested in the previous section were cloned into the prey pP6 plasmid, containing the GAL4 activating domain (AD). Six of them were inserted also to the bait pB27 plasmid, containing the LexA DNA binding domain (BD). The three remaining proteins (ARP4, RVB1, and PIE1) were not included in pB27 due to their complex cloning procedures.

The reporter gene in this system is HIS3, which encodes the gene for imidazoleglycerol-phosphate dehydratase, the product of which forms an enzyme required for synthesis of the amino acid, histidine (His). As such, physical interaction between the prey and bait proteins enable yeast cells (His^-) to proliferate on media lacking His. A positive control plate which contained His was used to test yeast growth while test plates that lacked His were used to test prey-bait interaction. Addition of 3-amino-1,2,4-triazole (AT) in the test plate, which marginally inhibits the synthesis of His [48], was used to assess the strengths of prey-bait interactions. The Y2H assay shows that SWC2 forms a homodimer and that two pairs of proteins, SWC6-SWC5 and YAF9-SWC2, display intermolecular interaction (Figure 3). The YAF9-SWC2 interaction was not apparent in the AT containing plate, suggesting a weak association between these proteins. The interaction between SWC6 and SWC5 has been previously published by Choi and colleagues [45], however some of the results in this report differ in that their Y2H assay revealed that SWC6 forms a homodimer and also interacts with SUF3 in

addition to SWC2. While it is unclear what contributed to the discrepancy it should be noted that the expression level of the proteins was not checked in my study. Additionally, a different Y2H system was used in the aforementioned study [45], which utilized a GAL4 BD instead of LexA BD. LexA BD is a popular choice to reduce false positives [49]. Alternatively, LexA BD-fused proteins may not bind to the intended reporter sequence, as previously reported [50]. It has also been shown that some protein interactions remain undetectable using one system over the other, depending on the proteins of interest [51]. Other results from Wu and colleagues [52] show that SUF3 and SWC6 are each dependent on the other for association with PIE1 as well as SWC2, suggesting that they form a subcomplex, which implies their direct physical interaction with each other. These results, however, were concluded from SDS-PAGE and silver staining, not with Y2H.

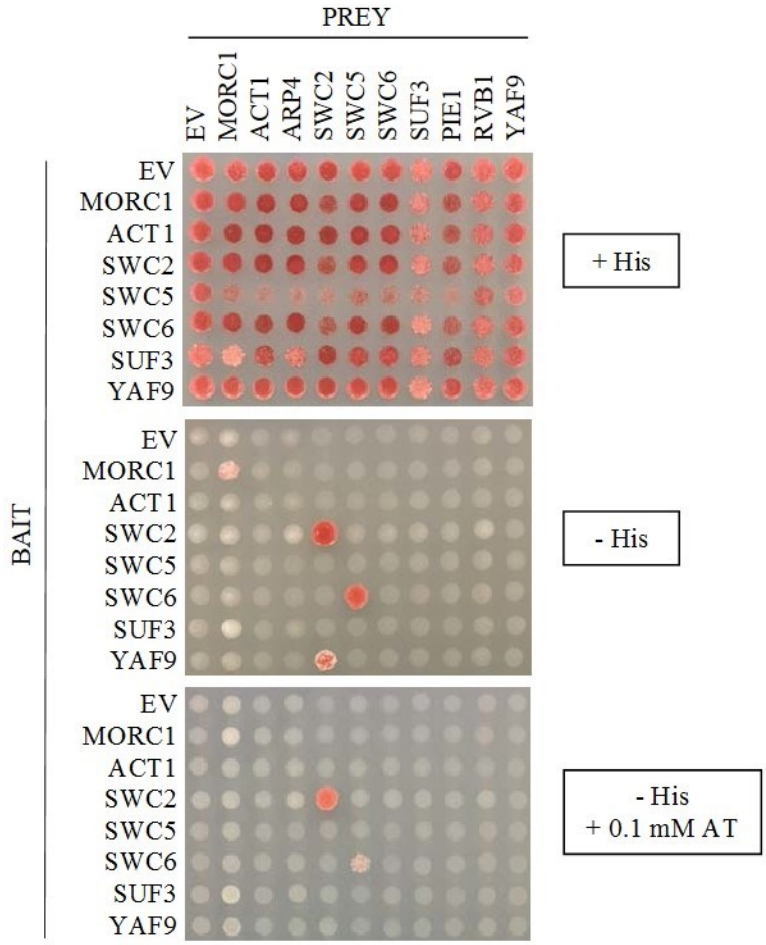

Figure 3. Yeast two-hybrid testing physical interactions among components of the SWR1-like complex and MORC1. Results indicate homodimerization of SWC2 and interaction between SWC6 with SWC5, and YAF9 with SWC2. 0.1 mM AT was used to inhibit the growth of yeast cells with weak prey-bait interaction. These results were repeated at least two times.

A separate Y2H was performed to test the interactions between the nine chromatin-remodeling factors and fourteen MORC1-interacting proteins (MIPs), which had previously been identified via Y2H using MORC1 as a bait and whose functions are indicated in Table 2. Given very little interaction between MORC1 and SWR1-like complex was found in Y2H, I hypothesized that MIPs screened through Y2H may function as a bridge mediating the interaction between MORC1 and SWR1-like complex. This experiment, however, revealed no significant interaction except for that of MIP14, weakly with SWC2 and even weaker with RVB1 (Figure 4a). Lack of interaction may be explained by the fact that full-length proteins, which were used in Figure 4a, often are not as interactive as their counterparts in a partial length, which were identified through the Y2H screening. A reason for this is often that in the truncated proteins, potential interacting domains may become exposed without being buried in a full-length protein, thus would be able to interact. For this reason, I also tested the chromatin-remodeling factors with partial-length MIPs in Figure 4b, which showed that the two interactions seen with the full-length set disappeared indicating that the portion of MIP14 that had been removed was fully or partially responsible for the interaction with SWC2 and RVB1. Note that none of the full-length MIPs except for MIP14 displayed interaction with MORC1 and only a subset of the partial-length MIPs showed interaction. This is likely due to the fact that MORC1 was used as the prey protein suggesting that some of MIPs do not show interaction when they were switched to the bait proteins. This lack of reciprocal interaction in Y2H is currently investigated.

Table 2. Fourteen MORC1-interacting proteins (MIPs) and their associated functions. 14 proteins were identified through Y2H using MORC1 as a bait.

	Annotation
MIP1	Intracellular protein transport;αSNAP2
MIP2	Response to heat; chloroplast-targeted HSP101 homologue
MIP3	MORC6
MIP4	CPL3 – functions as a negative regulator of abiotic stress-induced gene expression
MIP5	NAPP/WAVE – nuclear actin polymerizing. SNF chromatin remodeling factor
MIP6	Mitotic microtubule organizer
MIP7	Regulates proton transport
MIP8	SMC1 – involved in sister chromatid cohesion during DNA replication
MIP9	SANT – chromatin remodeling through histone tail-binding
MIP10	bZIP TF – transcription regulator, mediates defense, light signaling, seed maturation
MIP11	SNX1 – required for proper endosome-to-Golgi trafficking
MIP12	Carries the Mobile domain found in some WRKY transcription factors and some TEs
MIP13	Mediator complex protein
MIP14	COG6 – organizes vesicle targeting during intra-Golgi retrograde transport

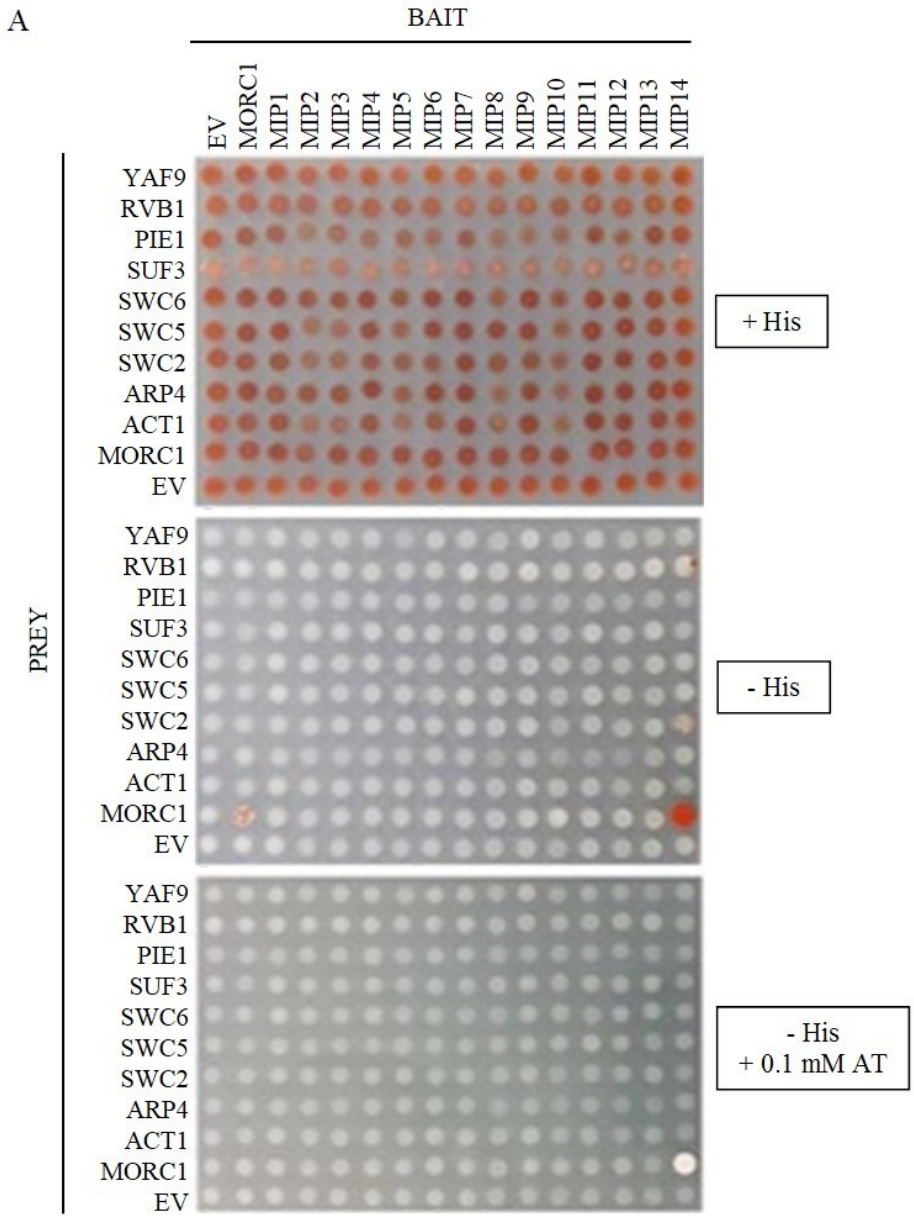

Figure 4. Very little physical interactions between components of the SWR1-like complex with MORC1 and MORC1-interacting proteins (MIPs) were found through Y2H. (A) Chromatin-remodeling factors tested with full-length MIPs. Interaction was found between MIP14 with SWC2, and MIP14 with RVB1. 0.1 mM AT was used to inhibit yeast growth in order to test for strength. All interactions listed are in order of decreasing strength. Note: the image of the 0.1 mM AT plate was taken two days prior to those of the +His and 0 mM AT plates, due to fungal growth contamination obscuring the quality of the results. The interactions however, displayed similar results from both days. (B) Chromatin-remodeling factors tested with partial-length MIPs. Weak interactions were found between the partially functional protein, MIP7, with SWC2 as well as with RVB1.

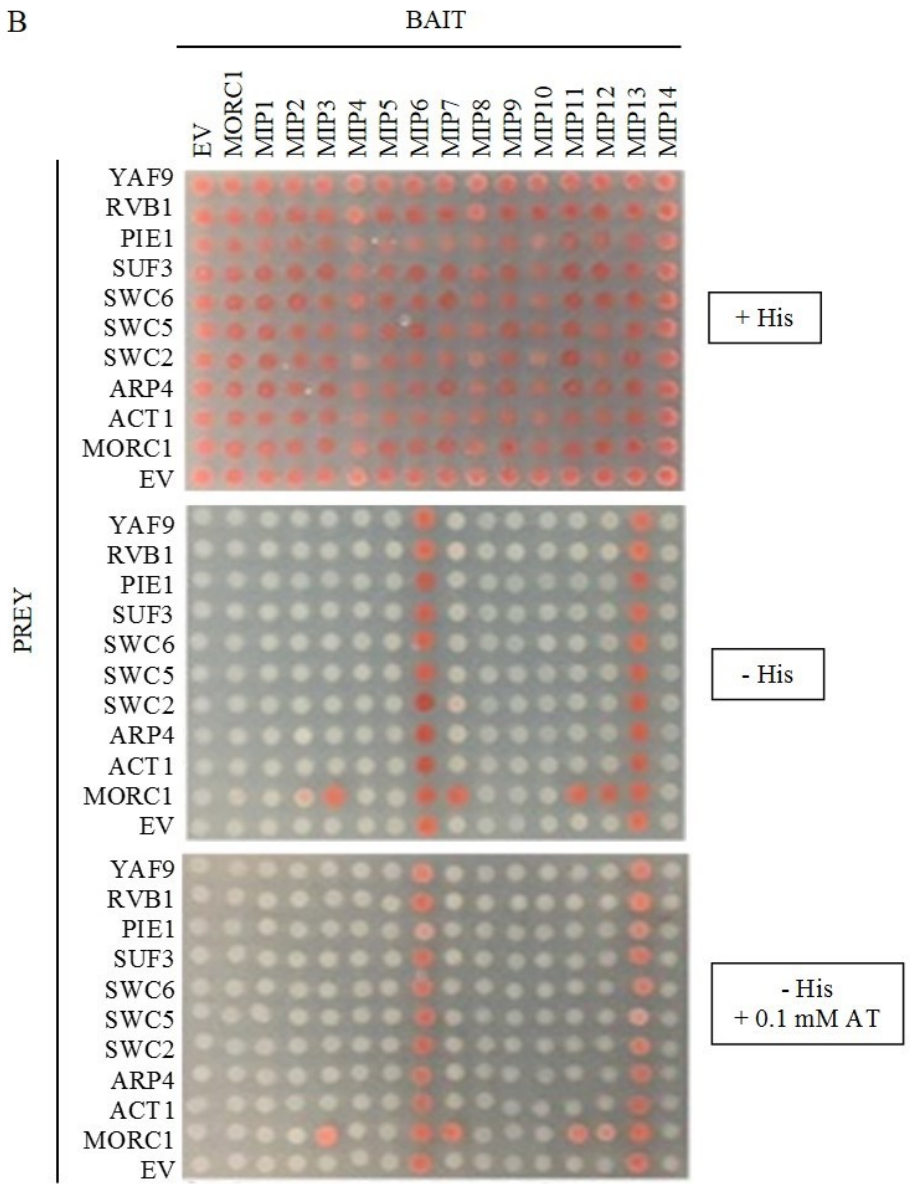

Figure 4, Continued. Very little physical interactions between components of the SWR1-like complex with MORC1 and MORC1-interacting proteins (MIPs) were found through Y2H. (A) Chromatin-remodeling factors tested with full-length MIPs. Interaction was found between MIP14 with SWC2, and MIP14 with RVB1. 0.1 mM AT was used to inhibit yeast growth in order to test for strength. All interactions listed are in order of decreasing strength. Note: the image of the 0.1 mM AT plate was taken two days prior to those of the +His and 0 mM AT plates, due to fungal growth contamination obscuring the quality of the results. The interactions however, displayed similar results from both days. (B) Chromatin-remodeling factors tested with partial-length MIPs. Weak interactions were found between the partially functional protein, MIP7, with SWC2 as well as with RVB1.

A reciprocal Y2H assay for RVB1-MORC1 was performed since it was initially not included in Figure 3. While this reciprocal Y2H did not reveal that MORC1 interacts with RVB1, it showed that RVB1, when fused with the LexA DNA binding domain, activates the His reporter (Figure 5a). To further narrow down a domain responsible for the auto-activation, five truncated RVB1 mutants were utilized (Figure 5b). While these truncated RVB1 proteins failed to interact with MORC1, an autoactivation was seen in the middle portion of RVB1 spanning amino acids 127-300. This observation suggests that this auto-activation may be suppressed when either the N- or C-terminal domain is present. The observation that RVB1 displays auto-activation only from the bait construct suggests that RVB1 may regulate transcriptional inductions. Indeed, the RVB1 protein was suggested to function as a transcriptional cofactor, which would help recruit transcription factors such as WRKY to enhance the transcription of target genes required for adequate R-protein mediated responses in plants [53]. Note that MORC1 is also shown to be a transcriptional cofactor when its truncated form was fused with the LexA BD (Nam and Kang, unpublished). Thus, these observations suggest that, while Y2H did not reveal the interaction between MORC1 and RVB1, they may perform function in plant immunity by modulating transcription induced by pathogen infection.

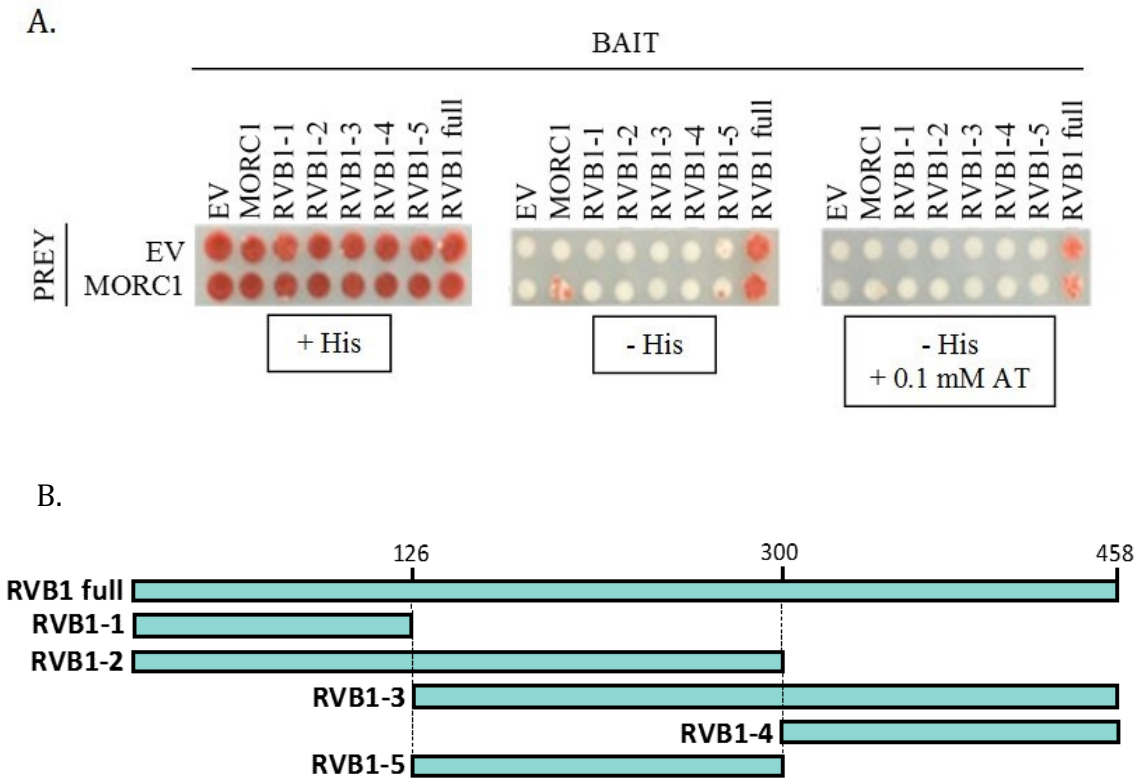

Figure 5: RVB1 bound to the bait construct exhibits auto-activation, of which the middle portion (amino acids 127-300) is partially responsible. (A) This Y2H indicates that RVB1, when bound to the reporter gene, causes auto-activation and that the middle portion of RVB1 consisting of amino acids 127-300, contains a constitutively active domain, which is negatively regulated by the presence of either the N or C terminus alone. (B) Diagram showing the relative portions of RVB1 in each construct (numbers indicate amino acids).

CHAPTER III

Histone variant H2A.Z, replaced by SWR1-like chromatin remodeling complex, plays a role in transcriptional activation of defense genes and immunity in Arabidopsis

Confirmation of Arabidopsis mutants for SWR1-like complex genes and generation of the combined mutants with *morc1/2*

T-DNA insertion lines of chromatin-remodeling factor mutants were obtained from the Arabidopsis Biological Research Center (ABRC) and their T-DNA insertion relative location in the gene is displayed in Figure 6, with the exception of the *suf3* mutant line, which was obtained through fast neutron mutagenesis [54]. The homozygous mutant genotype of each gene was confirmed and lines were subsequently crossed with *morc1 morc2* double-knockout mutants in which MORC1 and its closest homolog MORC2 are knocked-out [15]. These SWR1-like complex mutant plants with and without *morc1 morc2* were imaged with wild type (WT; Col-0) plants at three weeks after germination to assess their phenotypes. *arp4* displays a non-parental phenotype when crossed with *morc1 morc2* in that the leaves become curled (Figure 7). *suf3* and *swc5* both exhibited early flowering and the triple mutant *suf3 morc1 morc2* flowered even earlier (Figure 7). Taken together, these observations suggest that MORC1 may interact genetically with ARP4 and SUF3.

swc2 exhibits a dwarf phenotype (Figure 8), however this persists when combined with *morc1 morc2,* which does not support genetic interaction between MORC1 and

SWC2. A heterozygous line for *swc6 morc1 morc2* has a significantly prolonged lifespan, overall large leaves, and late flowering as compared to the WT (Figure 9a and b). Inflorescences were weak and flowers generally died upon emergence. These phenotypes were suppressed by incubating the plants at 16°C or by applying gibberellic acid. The F_1 progeny of *swc6* crossed with the single knockout mutant, *morc1* or *morc2*, also displayed similar phenotypes.

However, the *swc6* mutant is in the Col-3 background, whereas the *morc1, morc2,* and *morc1 morc2* mutants are in the Col-0 background. I therefore hypothesized that this potential genetic interaction may be due to hybrid-incompatibility, a condition in which the hybrid offspring exhibits heightened immune responses mostly leading to lethality through incompatible *R* genes [55]. In order to test this hypothesis, I crossed the *swc6* mutant line (in the background of Col-3) with the WT (Col-0). As a result, the F_1 progeny of the backcross, referred to as swc6/SWC6, Col-3/Col-0, revealed a similar phenotype as the F_1 progeny of the cross between *swc6* and *morc1 morc2* (Figure 9c). For this reason, we deduced that the phenotype observed in the swc6/SWC6, morc1/MORC1, morc2/MORC2 plants was not due to a genetic interaction between the proteins SWC6 and MORC1, but was a result of hybrid incompatibility between Col-3 and Col-0.

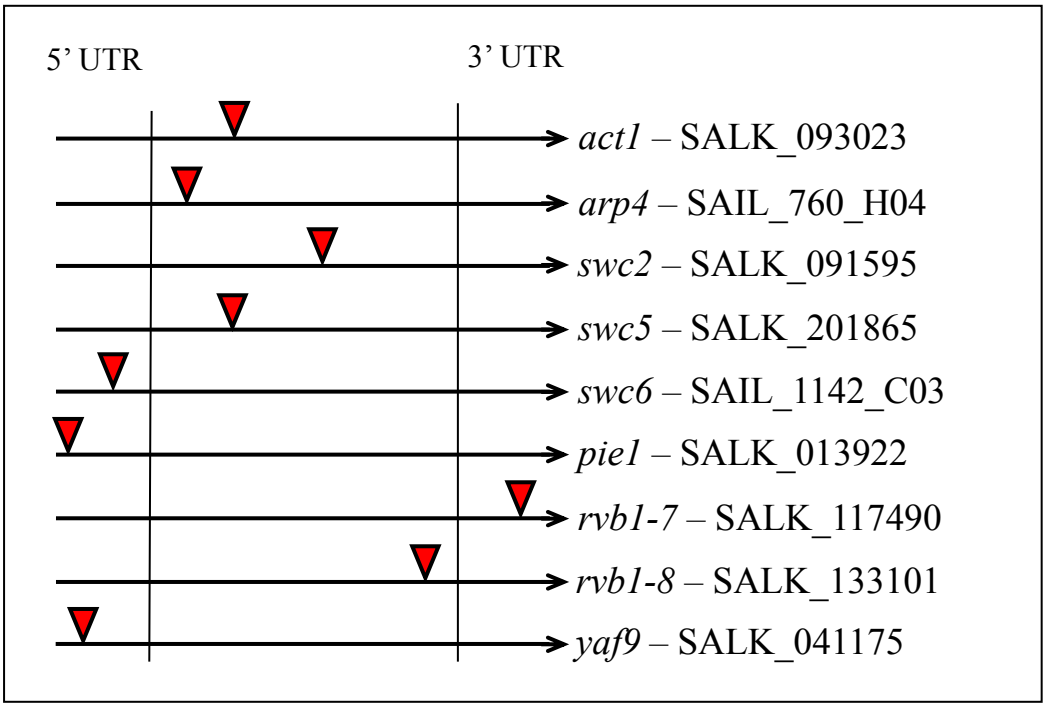

Figure 6. Relative position of T-DNA insertion along the gene. Red triangles indicate T-DNA insertion locations. First and second vertical lines indicate start and stop codons, respectively.

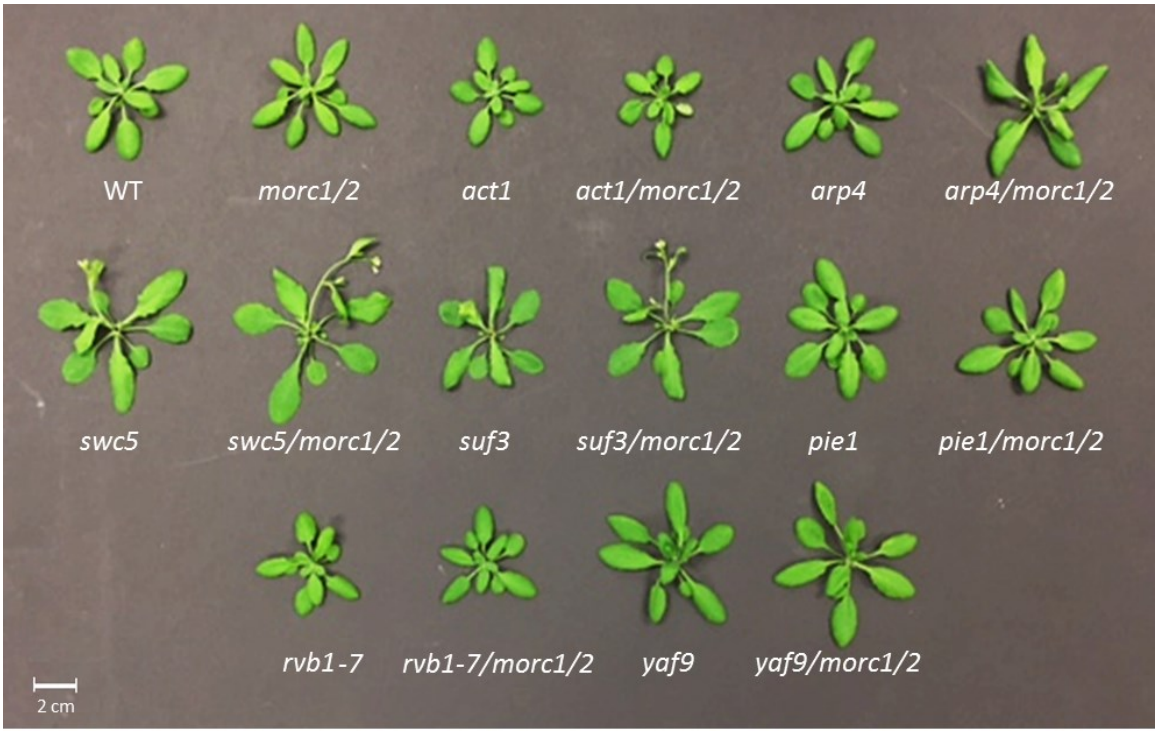

Figure 7. *arp4* and *suf3* mutant plants displayed non-parental phenotypes when combined with *morc1 morc2*. SWR1-like complex mutant plants with and without *morc1 morc2* were imaged with wild type (WT) plants at three weeks after germination to assess their phenotypes which were compared to those of parental WT (Col-0) and *morc1/2*. Note: scale bar indicates 2 cm.

Figure 8. *swc2* exhibits a dwarf phenotype as compared to WT (Col-0). Three *swc2* homozygous plants indicated by red circles displaying a dwarf phenotype alongside WT (Col-0) plants.

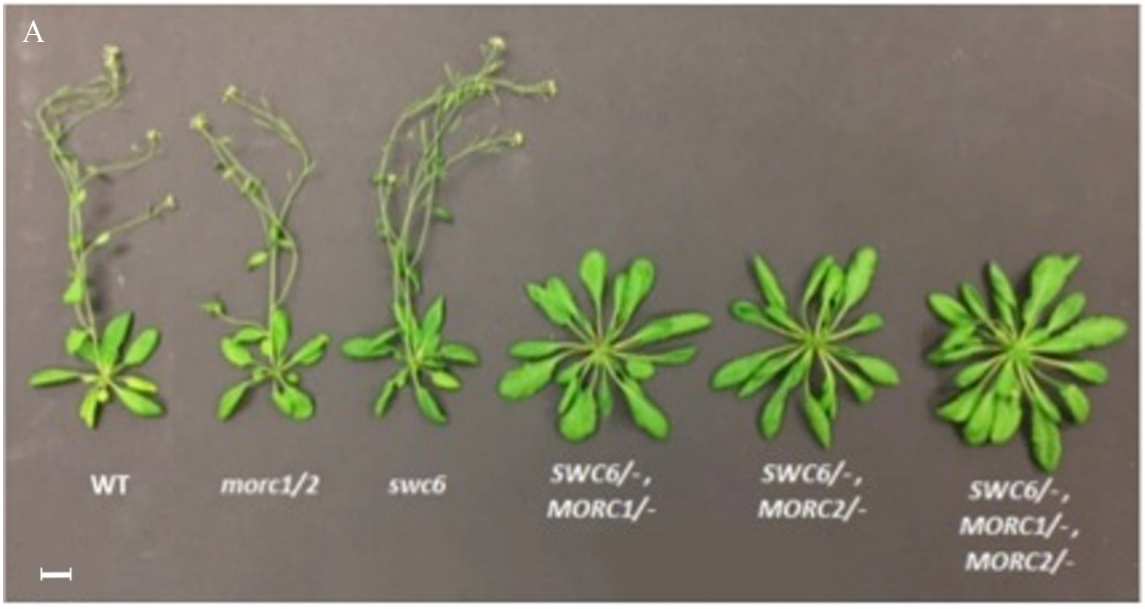

Figure 9. The *swc6/SWC6 morc1/MORC1 morc2/MORC2* phenotype is a result of hybrid incompatibility between Col-0 and Col-3. (A) The phenotype of *swc6/SWC6 morc1/MORC1 morc2/MORC2* showed late flowering, larger leaves, and (B) a prolonged lifespan. Plants on the left are 6 weeks old and plants on the right are 21 weeks old. (C) *swc6/SWC6, Col-3/Col-0* shows a similar phenotype as *swc6/SWC6, morc1/MORC1, morc2/MORC2*, suggesting that this phenotype is associated with hybrid incompatibilty, the result of the cross between the Col-3 and Col-0 genetic backgrounds. Note: scale bar indicates 2 cm.

The suppression of the *RVB1* gene in Arabidopsis proves lethal, and so the gene cannot be completely knocked out [27, 45]. As such, we used an *rvb1-7* mutant whose T-DNA insertion is located in the 3' UTR (SALK_117490) (Figure 10a). I hypothesized that this *rvb1-7* mutant was a knock-down mutant, to an extent. Semi qRT PCR (quantitative Reverse Transcriptase Polymerase Chain Reaction) analysis revealed, however, that the transcript level of *RBV1* in *rvb1-7* is comparable to that in the WT, suggesting that there is less likely significant reduction of the RVB1 protein in the mutant line (Figure 10b). These results were confirmed by qRT-PCR, which indicates that the *rvb1-7* mutant expresses slightly higher levels of *RVB1* than its WT plants (Figure 10c).

Due to this result, it became apparent that the *rvb1-7* line was not suitable for further study. Instead, another T-DNA insertion line (SALK_0133101), with the insertion located before the stop codon of coding sequence, was tested (Figure 11a) and named *rvb1-8*. As anticipated, no homozygous mutants were identified, suggesting that this mutation is lethal. Semi qRT PCR and qRT PCR showed that the transcription of *RVB1* in *rvb1-8/+* was significantly lower than that of the WT (Figure 11b and c). As such, we continued to use this line for my study.

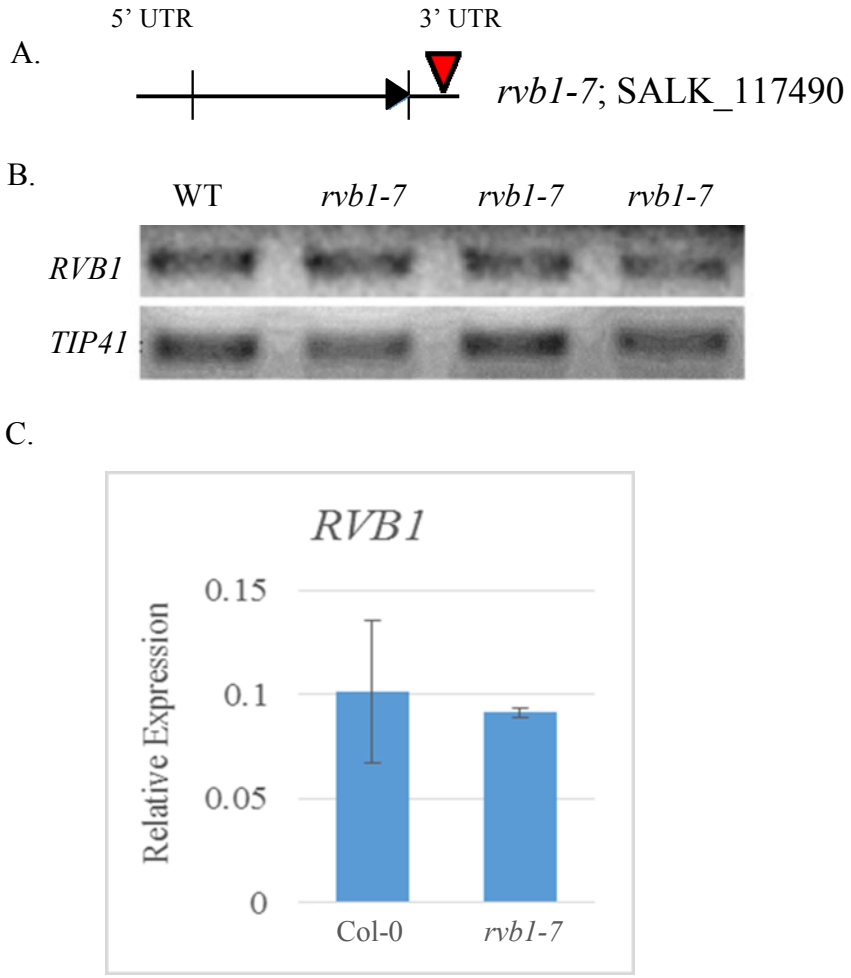

Figure 10. The *rvb1-7* line (SALK_177490) does not have lower mRNA levels than the wild type. (A) Relative location of the T-DNA insertion. First and second vertical lines indicate start and stop codons, respectively. (B) Semi-quantitative RT-PCR results indicated that the *RVB1* gene in the mutant is not knocked out or down, and in fact displayed a level comparable to that of WT**.** The *Tip41-like* gene was used as a control. (C) qRT-PCR results indicated that *rvb1-7* exhibits similar or slightly elevated levels of *RVB1* mRNA. Two additional replicate experiments were performed with similar results. No significant difference was found between WT and *rvb1-7.*

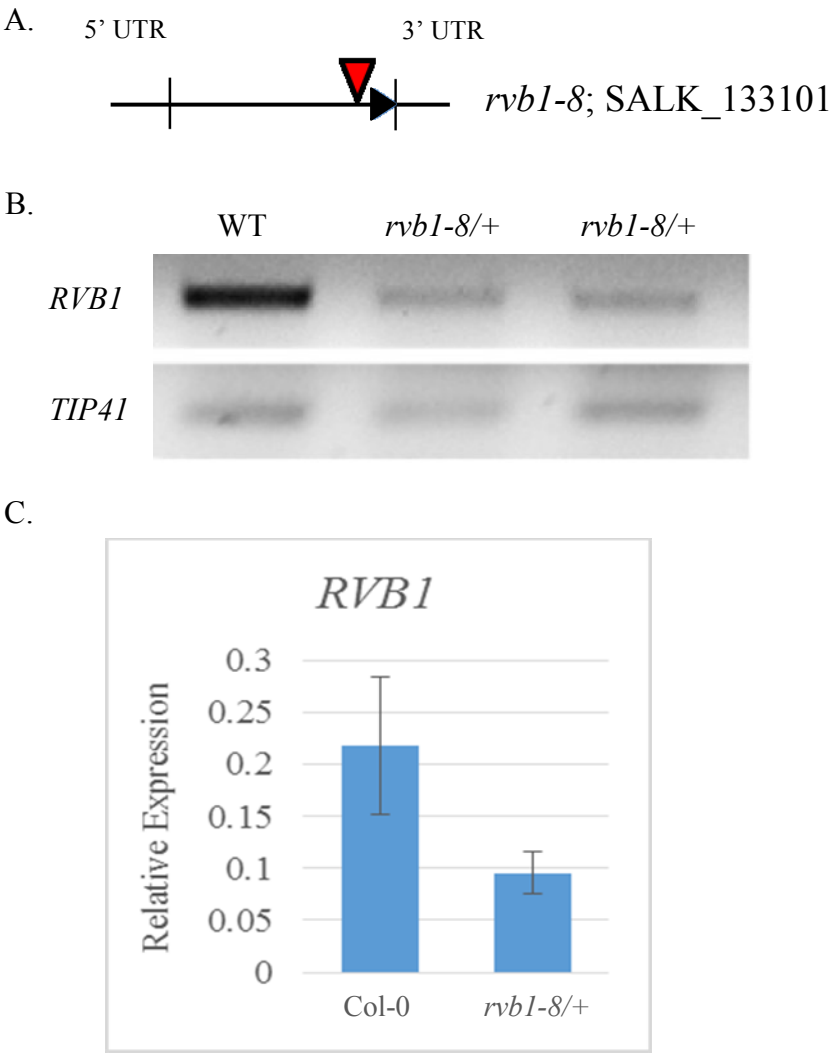

Figure 11. The *rvb1-8* line (SALK_0133101) is a knock-down mutant. (A) Relative location of the T-DNA insertion. First and second vertical lines indicate start and stop codons, respectively. (B) Semi-quantitative RT-PCR suggests that the expression of *RVB1* in heterozygote *rbv1-8/+* is considerably reduced as compared to WT. Two independent lines are presented. *Tip41-like* was used as a control. (C) qRT-PCR results confirm that *rvb1-8/+* exhibits a significantly reduced level of *RVB1*. This experiment contained three biological replicates. Asterisks indicate statistically significant differences (**$P<0.01$, t-test) between mutants and WT.

Some of the mutants for the SWR1-like complex display altered resistance to *Pst*

As most of the chromatin-remodeling factors exhibit indirect physical interaction with MORC1, an important regulator in plant immunity, I analyzed resistance in the mutants generated above against *Pst* carrying the luminescent *luxCDABE* reporter gene with and without *AvrRpt2*, which is an effector triggering ETI in Arabidopsis. This reporter was used to measure bacterial resistance in a large-scale from images taken 2 days post-infection (2dpi) for both *Pst*- as well as *Pst (avrRpt2)*-treated plants [56]. The experiment was replicated at least three times, with all replicates showing a similar trend (Figures 12 and 13).

Results indicate that *arp4, swc5, suf3, pie1,* and *yaf9* are compromised in resistance (Figure 12). Similarly, a study by Cheng et al. shows that *suf3* has compromised resistance to avirulent *Pst* [57]. This suggests that ARP4, SWC5, SUF3, PIE1, and YAF9 may be involved in resistance against *Pst* in Arabidopsis. Interestingly, introduction of *morc1 morc2* to *swc5, suf3,* and *pie1* recovered compromised resistance found in their single mutants; note that *morc1 morc2* also has reduced resistance. This raises the possibility that genetic interaction of MORC1 with SWC5, SUF3, and PIE1 may be antagonistic rather than additive or synergistic. The *yaf9 morc1 morc2* mutant was the only one to display further increased susceptibility to *Pst* as compared to the *yaf9* parental line.

The *rvb1-8/+* heterozygote line was tested for resistance against avirulent *Pst* carrying *avrRpt2* along with *rvb1-8/+ morc1 morc2*; I learned that the reporter based resistance assay in Figure 12 is not sensitive enough for avirulent *Pst* carrying *avrRpt2* which grows slower by ETI in Arabidopsis as compared to virulent *Pst*. However, *morc1*

morc2 displays a bigger difference in ETI as compared to PTI [15], which justifies testing the ETI instead. As the plants were heterozygous for *RVB1*, they were genotyped after checking the resistance for each individual plant. Oddly, the ratio of heterozygotes among the population was not an expected 2:1 segregating population of heterozygotes to WT as *rvb1-8* homozygous plants are not viable. In fact, after screening a total of 145 plants, the mutants exhibited a 3:4 ratio of heterozygotes to WT, suggesting that perhaps some heterozygotes are lethal. In addition, the heterozygote *rvb1-8/+* plants displayed a high level of variation with regard to plant resistance against avirulent *Pst* carrying *avrRpt2*. Although the pattern shown in Figure 14 was not reproduced consistently among replicates, it represents the overall trend among 10 replicates, where *rvb1-8/+* displayed increased susceptibility to avirulent *Pst* carrying (*avrRpt2*) as compared to WT and *rvb1-8/+ morc1 morc2* displayed increased resistance compared to *rvb1-8/+* alone. The variation in resistance among heterozygous plants was observed because epigenetic mutations often lead to a variety of other changes in genome [58], most of which occur at random.

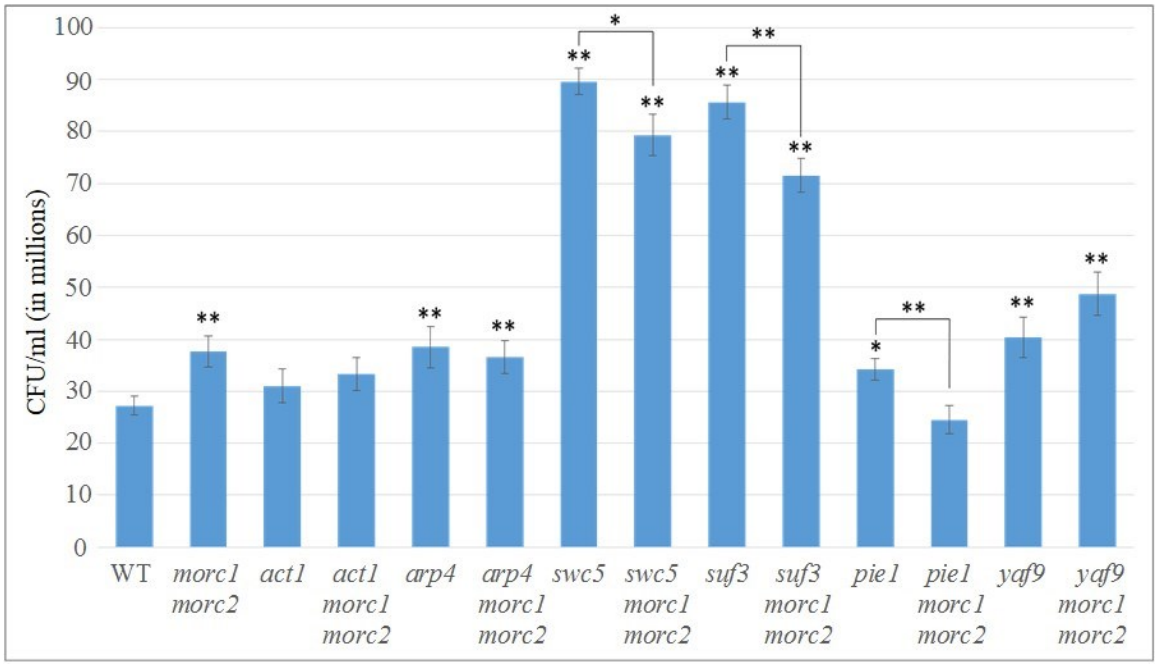

Figure 12. Resistance of single and triple mutants compared to parental lines against virulent *Pst*. Of the single mutants tested, *arp4, swc5*, *suf3, pie1,* and *yaf9* show greater susceptibility than WT (Col-0) to virulent *Pst*. The triple mutants, *swc5 morc1 morc2*, *suf3 morc1 morc2,* and *pie1 morc1 morc2* show increased resistance compared to their single mutants, *swc5, suf3* and *pie1*, and these results are statistically significant. This trend has been replicated three times. Experiments were done three times with similar results. Asterisks above blue bars indicate statistically significant differences (***P*<0.01, **P*<0.05, t-test) between mutants and WT. Asterisks in a pairwise comparison above a line shows significant difference (**P<0.01, *P<0.05, t-test) between the indicated pair.

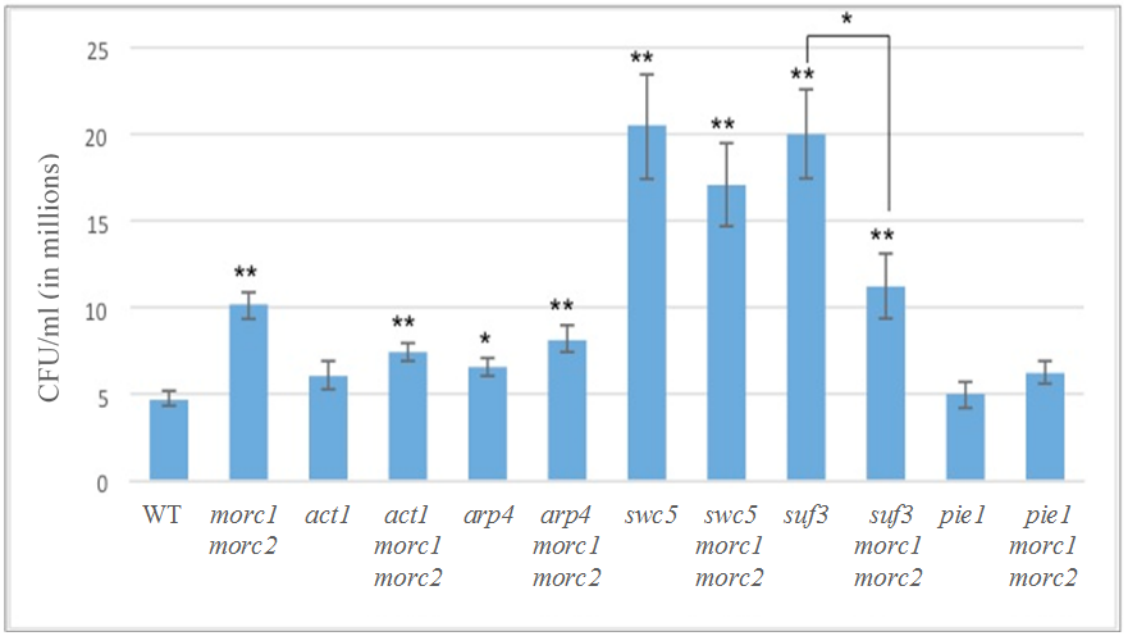

Figure 13. Resistance of single and triple mutants compared to parental lines against avirulent *Pst*. Of the single mutants tested, *arp4, swc5,* and *suf3* show greater susceptibility than WT (Col-0) to *Pst (avrRpt2)*. The triple mutant *suf3 morc1 morc2* shows significantly increased resistance compared to the single mutant, *suf3*. This pattern has been repeated three times and the results of yaf9 are not shown as its pattern was not repeated. Experiments were done twice with similar results. Asterisks indicate statistically significant differences (***P*<0.01, **P*<0.05, t-test) between mutants and WT. Asterisks in a pairwise comparison above a line shows significant difference (**P<0.01, *P<0.05, t-test) between the indicated pair.

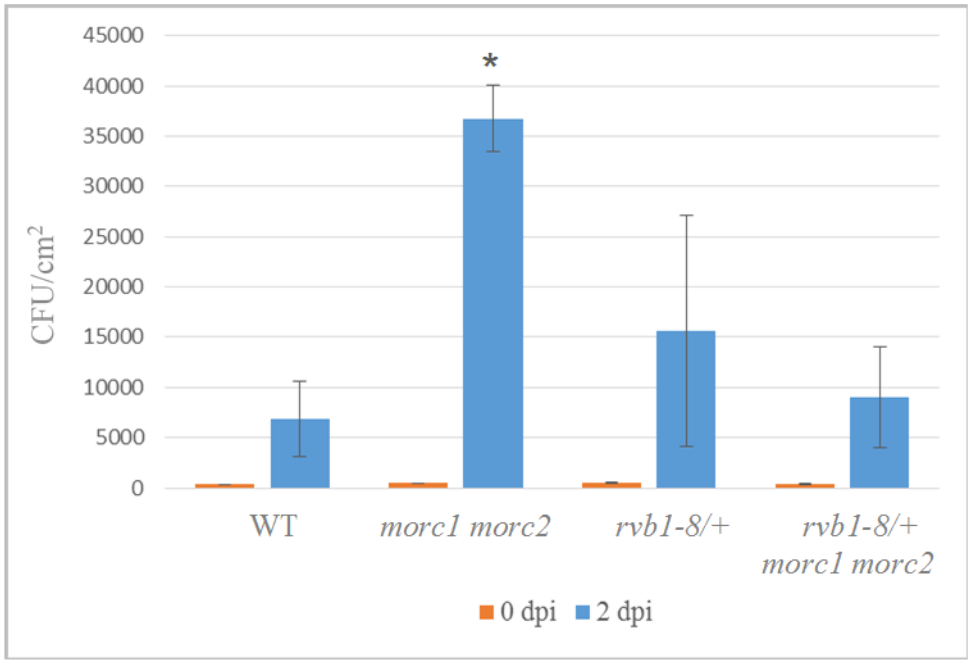

Figure 14. Resistance of *rvb1-8/+* and *rvb1-8/+ morc1 morc2* against avirulent *Pst.* The heterozygote *rvb1-8/+* displayed slightly lower level of resistance against *Pst (avrRpt2)* as compared to WT, with high variation, and the *rvb1-8/+ morc1 morc2* line showed more resistance than *rvb1-8/+*. Asterisks indicate statistically significant differences (**P<0.01, *P<0.05, t-test) between mutants and WT.

MORC1 interacts with RVB1 in both the nucleus and microsomes

RVB1 is an essential protein [27, 45] which is associated with the RNA polymerase II holoenzyme, telomerase complex, microtubules during cell division and Rab5 in endosomes to support Ras-mediated endocytosis [40-42, 44]. As it has nuclear as well as non-nuclear functions, the interaction site at the subcellular level between MORC1 and RVB1 was further analyzed. As MORC1 predominantly resides in microsomes and a small subpopulation exists in the nucleus [15], it was hypothesized that the interaction between RVB1 and MORC1 occurs in the nucleus, as both proteins play a role in epigenetic regulation [14, 16, 17, 19, 22, 23, 36], however it did not exclude the possibility of a non-nuclear interation. To test this hypothesis, we performed subcellular fractionation on *N. benthamiana* tissue infiltrated with Agrobacteria containing *RVB1-FLAG* and *Myc-MORC1*; *GFP-FLAG* in place of *RVB1-FLAG* was used as a negative control. The resulting nuclear, microsomal, and cytosolic fractions were then subjected to Co-IP in which agarose beads conjugated to the anti-FLAG antibody was used to immunoprecipitate FLAG-tagged proteins.

The results of the Co-IP indicate that MORC1 and RVB1 interact in both the nucleus and microsomes. RVB1 co-localizes with Rab5 on endosomes for Ras-mediated endocytosis, and therefore its presence in microsomes is not surprising [44]. Physical interaction of MORC1 and RVB1 in both the nucleus and microsomes therefore suggests that the cellular role(s) played between MORC1 and RVB1 may not be limited to chromatin remodeling and therefore further experiments would be necessary to characterize the non-nuclear function. Antibodies against histone H3 and PEPC (phosphoenolpyruvate carboxylase) that are specific to the nucleus and cytosol,

respectively, were used as controls to ensure that the subcellular fractionation was performed properly.

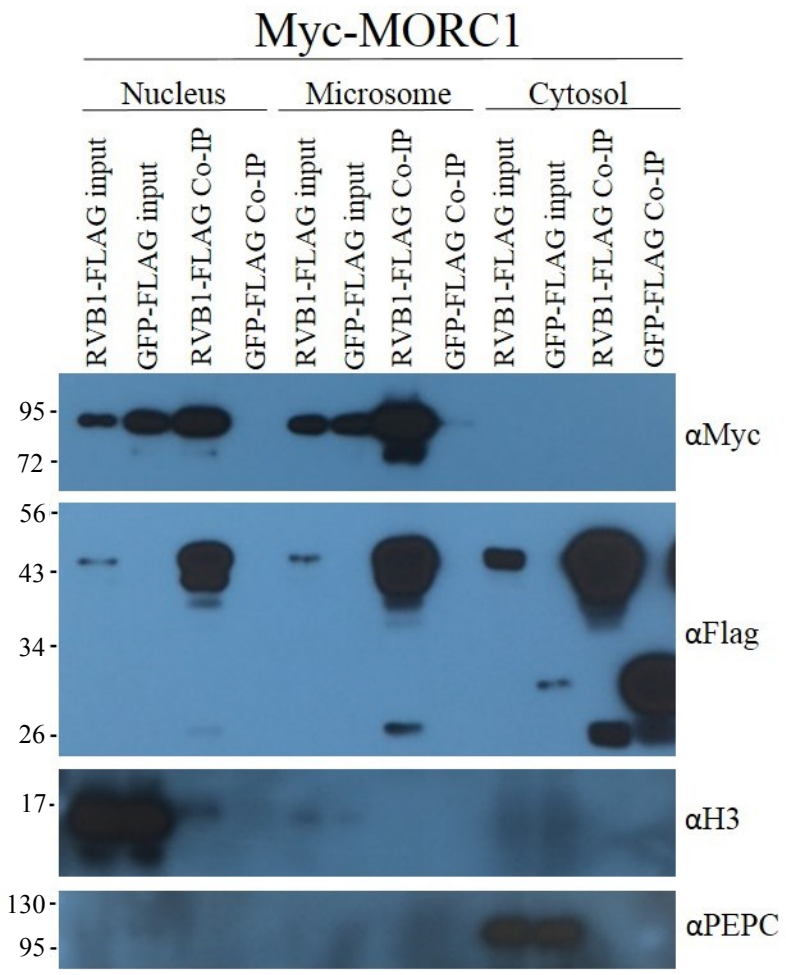

Figure 15. MORC1 interacts with RVB1 in the nucleus and microsomes. Subcellular fractionation on *N. benthamiana* tissue infiltrated with Agrobacteria containing *RVB1-FLAG* and *Myc-MORC1* was performed; *GFP-FLAG* in place of *RVB1-FLAG* was used as a negative control. The resulting nuclear, microsomal, and cytosolic fractions were then subjected to Co-IP in which agarose beads conjugated to the FLAG antibody was used to immunoprecipitate FLAG-tagged proteins. Antibodies against histone H3 and PEPC (phosphoenolpyruvate carboxylase) were used as controls for the nucleus and cytosol, respectively.

The level of histone variant H2A.Z associated with chromatin is elevated in response to infection with *Pst*

Chromatin-immunoprecipitation (ChIP) was performed using a transgenic plant containing both H2A.Z tagged with BLRP (biotin ligase recognition peptide), as well as the *E. coli* biotin ligase, BirA [29] to assess the replacement of H2A with its variant H2A.Z. This variant is deposited on gene bodies of responsive genes, thereby supporting the role that H2A.Z plays in moderating transcription inductions [30]. Interestingly, ChIP with H2A.Z recovered considerably more DNA when the *H2A.Z-BLRP* plants were challenged with *Pst* as compared to the mock control (Figures 16 and 17), suggesting that pathogen infection induces the replacement of H2A.Z.

H2A.Z was shown to be deposited on gene bodies of responsive genes [30]. Thus, I tested a few defense genes whose transcription is highly induced by pathogen infection to see if H2A.Z replacement is associated with these inducible genes. To this end, I performed ChIP using streptavidin-conjugated magnetic beads on tissue infiltrated with 10^6 cfu/ml virulent *Pst* as well as avirulent *Pst* carrying *avrRpt2* after 24 hours compared to mock treated tissue. The extracted DNA was then subjected to semi-qPCR (semi-quantitative PCR) using primers specific to genic as well as promoter regions of *PR-1, PR-2,* and *PR-5.* The presence of a band in the BLRP-H2A.Z line in Figure 16 indicates that H2A.Z was deposited in the region amplified by the primers, suggesting that H2A.Z was deposited in defense-related genes including *PR-1, PR-2,* and *PR-5* following pathogen attack. However, it should be also noted that reference genes such as *TIP41-like*, *UBC*, and *ACT2* in which their expression does not change significantly in response

to pathogen infection [59], also have significant H2A.Z deposition, suggesting that this variant replacement may be global.

A mutant deficient in H2A.Z variant displays altered expression of defense genes in response to pathogen infection

A mutant *h2a.z* line, which has three genes comprising H2A.Z knocked out – *hta8*, *hta9*, and *hta11* was tested to their function in plant immunity. The *h2a.z* mutant displayed a dwarf phenotype with early flowering, suggesting that these genes are also involved in plant development. To test transcriptional induction of defense genes in the histone variant deficient line, the *h2a.z* mutant was infiltrated, along with its WT plants, with mock (10 mM $MgCl_2$) or 10^6 cfu/ml of virulent *Pst* at 2.5 weeks of age, prior to flowering. Tissue from each line was collected at 6, 24, 48, and 72 hours post infection (hpi) as well as non-treated (naïve) tissue. RNA was extracted from the tissue and converted to cDNA (complementary DNA) and subjected to qRT-PCR using primers specific to defense-related genes, namely *PR-1, PR-2,* and *PR-5.* The relative expression of these genes in *h2a.z* compared to WT are shown in Figure 18 and demonstrate that there is a difference of gene inductions between these two lines. In the case of *PR-1* and *PR-2,* the *h2a.z* mutant line shows reduced expression at 48 hpi compared to WT, which is statistically significant in the case of *PR-1.* This trend persists at 72 hpi in the case of *PR-2* gene expression. The relative expression of *PR-5* however is greater in the *h2a.z* mutant compared to WT at 48 hpi. It is unclear why the induction of *PR-1* and *PR-2* is compromised and that of *PR-5* is enhanced in response to *Pst*. Nonetheless, these results suggest that H2A.Z is likely involved in regulating the transcriptional inductions of

defense-related genes upon pathogen attack although how general this involvement is would be remained to be characterized.

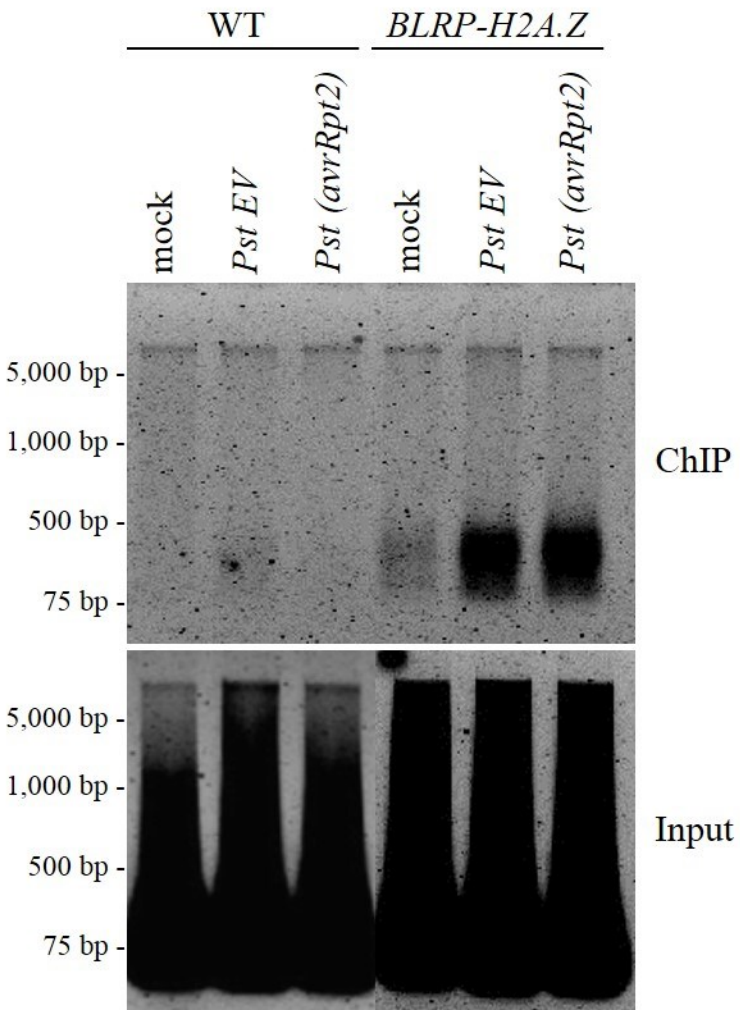

Figure 16. The genome-wide deposition of H2A.Z increases after pathogen infection. DNA from the input and ChIP samples were loaded on a 2% agarose gel and stained with SYBR green and imaged using a Typhoon scanner. The bands shown in the BLRP-H2A.Z samples indicate that the ChIP worked sufficiently.

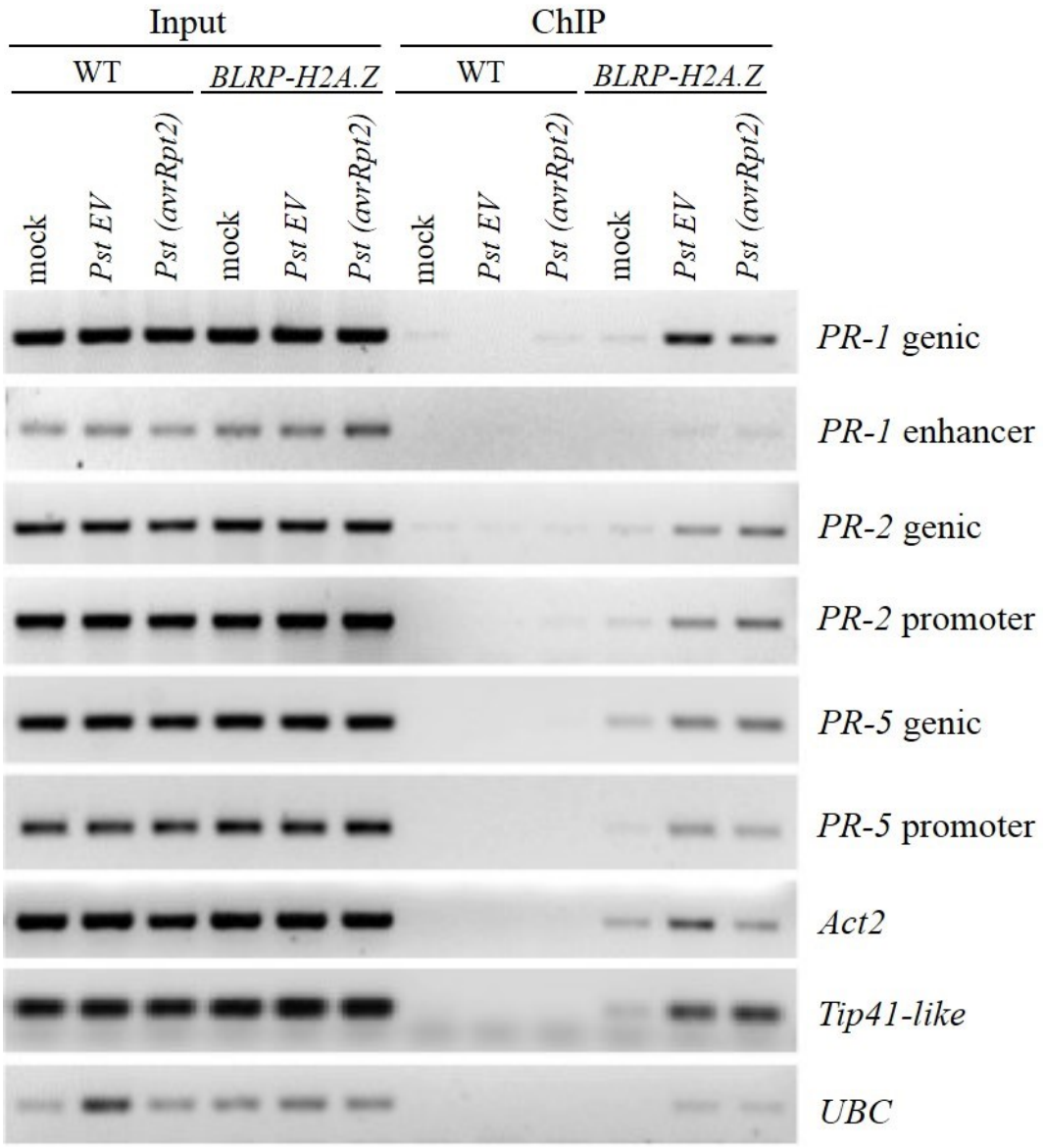

Figure 17. Chromatin immunoprecipitation (ChIP) reveals that H2A.Z is deposited on defense genes and some housekeeping genes in response to pathogen infection. ChIP was performed by using streptavidin-conjugated magnetic beads on mock treated tissue as well as tissue infiltrated with virulent *Pst* or avirulent *Pst* carrying *avrRpt2* after 24 hours (10^6 cfu/ml). The extracted DNA was subjected to semi-qPCR (semi-quantitative PCR) using primers specific to genic as well as promoter regions of *PR-1, PR-2,* and *PR-5.* The presence of a band in the BLRP-H2A.Z line indicates that H2A.Z was deposited in the region amplified by the primers. Housekeeping genes such as *TIP41-like*, *UBC*, and *ACT2* were tested.

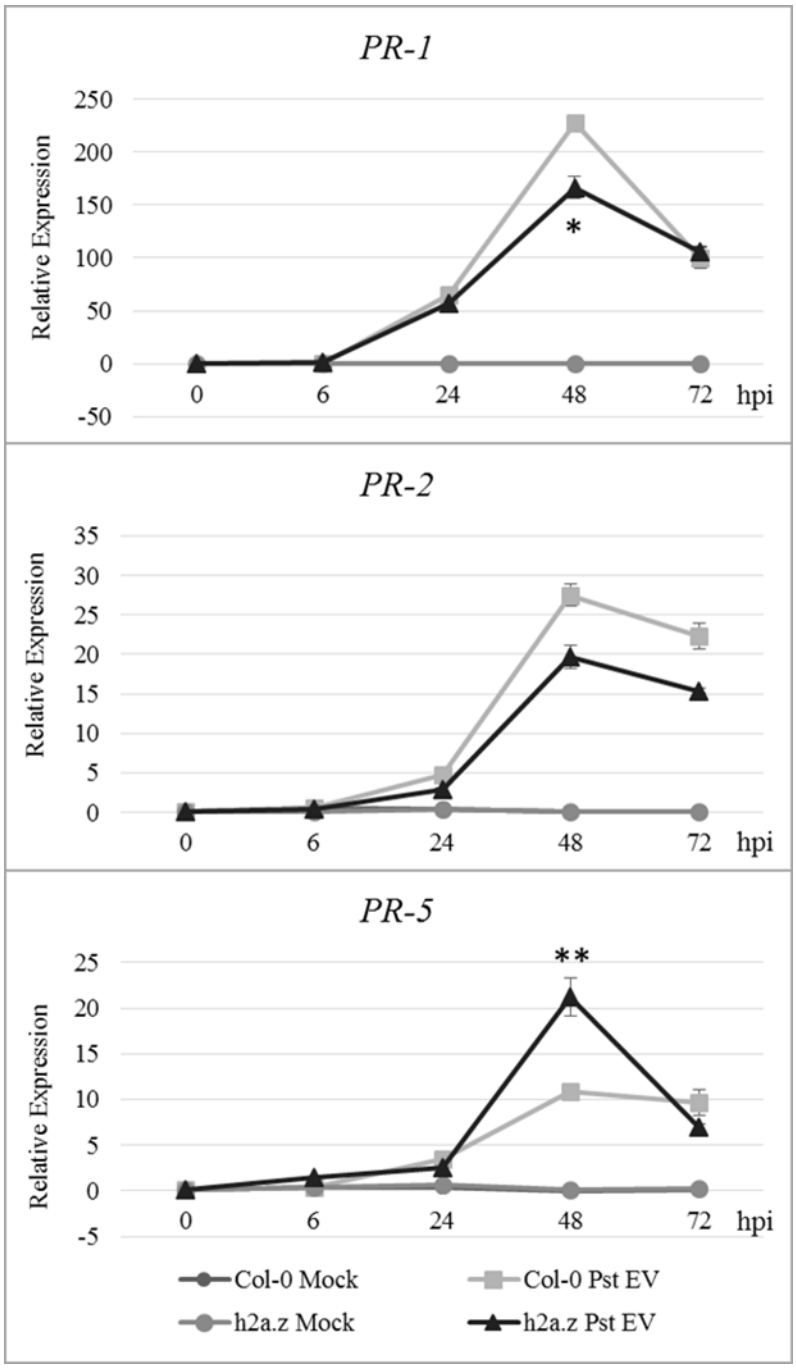

Figure 18. The *h2a.z* mutant shows altered transcription induction of defense-related genes. The *h2a.z* mutant plants were infiltrated, along with their WT plants, with mock (10 mM $MgCl_2$) or 10^6 cfu/ml of virulent *Pst* at 2.5 weeks of age, prior to flowering. Tissue from each line was collected at the indicated hours post infection (hpi) as well as non-treated (naïve) tissue. RNA was extracted from the tissue and converted to cDNA (complementary DNA) and subjected to qRT-PCR using primers specific to the *PR-1, PR-2,* and *PR-5* defense genes. Experiments were done twice with similar results. Asterisks indicate statistically significant differences (**P<0.01, *P<0.05, t-test) between mutants and WT receiving the same treatment.

CHAPTER IV

Potential functions of SWR1-like chromatin-remodeling factor complex and the increase of H2A.Z deposition in plant immunity

MORC1 has been shown to be required for ideal levels of plant immunity against a variety of pathogens including turnip crinkle virus and *Pst* [13, 15]. It has shown to be involved in chromatin condensation; this role of MORC1 in epigenetics was recently identified in an independent mutant screening to search for players in gene silencing [16]. My research reveals that, apart from the role of MORC1 in chromatin condensation [16], MORC1 physically associates with a majority of the protein components that comprise the SWR1-like complex including ACT1, ARP4, SWC2, SWC6, SUF3, PIE1, RVB1, and YAF9. The SWR1-like complex in Arabidopsis is analogous to the yeast SWR1 complex [27, 36], which is a chromatin-remodeling machinery that functions to replace histone H2A for H2A.Z [19, 22]. This replacement has been speculated to be involved in transcriptional regulation as it occurs in the promoter and/or genic region of actively transcribed genes [30]. Therefore, the physical interaction between MORC1 and SWR1-like protein components further supports the notion that MORC1 may be involved in chromatin remodeling and epigenetic regulation of gene transcription.

The resistance assay performed in this study revealed that the *swc5* and *suf3* mutants are highly susceptible to pathogen infection, however when crossed with *morc1 morc2,* their resistance was restored. This does not follow a typical synergistic or additive effect whereby loss of two components necessary for immunity would render the plant more susceptible than single mutants. This phenomenon was observed in both the

virulent as well as avirulent *Pst* treated plants, indicating a complex genetic interaction between MORC1 with SWC5 and SUF3. The genetic interaction between MORC1 and SUF3 was not limited to the resistance phenotype since the *suf3 morc1 morc2* triple mutant flowered significantly earlier than the *suf3* mutant, which itself displays an early flowering phenotype. In addition, the *arp4 morc1 morc2* triple mutant exhibited curly leaves, whereas the *arp4* single mutant did not, suggesting an extended genetic interaction between MORC1 with ARP4 beyond plant immunity.

RVB1 is a chromatin-remodeling factor that forms a heterodimer with RVB2 in the SWR1-like complex. However it has also been shown that RVB1 acts as a negative regulator of plant immunity [38]. This dual-function of RVB1 working as a chromatin-remodeling factor with implications in plant immunity prompted me to further explore the relationship between RVB1 and MORC1, which itself has dual association in epigenetic regulation and plant immunity. In order to identify where the two proteins interact at the subcellular level, I performed a Co-IP using subcellular fractions of plant tissue and found that MORC1 and RVB1 physically interact in the nucleus as well as microsomes, which suggest that the relationship between MORC1 and RVB1 may not be limited to chromatin remodeling. In the cell, MORC1 predominantly resides in microsomes. However, a subpopulation in the nucleus increases in response to biotic stress [14]. RVB1 functions in the nucleus as a chromatin-remodeling factor and co-localizes with Rab5 in endosomes to support Ras-mediated endocytosis [44]. The transgenic lines used for this experiment incorporated *RVB1* and *MORC1* under an estradiol-inducible promoter, and therefore may not fully represent the natural condition of interaction between the two proteins. As such, this method should be repeated using

transgenic lines that express *RVB1* and *MORC1* under their native promoters. Additionally, a bimolecular fluorescence complementation assay (BiFC) that visually reveals the subcellular localization of interaction will be a complementary tool for the Co-IP results presented (Figure 15). Also, given that MORC1 in the nucleus increases in response to *Pst* infection, it will be interesting to see if biotic stress changes the profile of MORC1-RVB1 interaction at the subcellular level.

A study by Brickner et al. supports that H2A.Z may be involved in transcriptional memory by; i) binding to chromatin encompassing those genes which have been recently transcribed in response to stress and ii) by positioning the gene near the nuclear periphery for rapid reactivation, which can persist for several generations [60]. The information described above was obtained using a eukaryotic yeast system and has not been tested in plants. Transcriptional memory itself however has been documented in plants, through histone modifications such acetylation and methylation of lysine residues on histones H3 and H4, whereby a variety of WRKY transcription factors are primed to induce a stronger defense response in a subsequent and comparable stress event [61]. Based on our results together with finding in yeast [60], it is tempting to speculate that H2A.Z may also be involved in transcriptional memory in plants.

My results in Figure 18 suggest that the deposition of H2A.Z might affect the expression of defense-related genes under biotic stress. I analyzed the relative expression of *PR-1, PR-2,* and *PR-5* after pathogen infection at different time points and found that for all genes, the pattern of expression differed in *h2a.z* mutants as compared to WT, which was especially pronounced at 48 hpi. Coleman Derr et al. 2012 have previously performed ChIP-seq on the *h2a.z* mutant line and reported that H2A.Z deposition in gene

bodies regulates the responsiveness of genes [30]. My study is the first demonstration that H2A.Z deposition changes in response to pathogen infection, suggesting that this histone variant replacement plays a role in transcriptional regulation. As its deposition occurs on defense-related genes such as *PR-1, PR-2, and PR-5* in response to pathogen infection, it seems highly likely that it would play a role in epigenetic regulation of plant immunity, however its specificity on defense genes remains to be tested. As such, this observation merits a genome-wide ChIP-seq analysis in order to analyze replacement of H2A.Z under biotic stress at a system level, which is currently underway. This information would provide an overall picture of H2A.Z deposition in plant genomes in response to stress, not limited to defense-related genes, but perhaps other responsive genes and transposable elements as well, which are widely induced under pathogen stress [62, 63]. In summary, I have identified physical interaction between MORC1 and a majority of the SWR1-like components and identified potential genetic interactions between MORC1 with SWC5, SUF3, and ARP4. I also have shown that several SWR1-like components display altered levels of resistance to pathogen attack, providing another novel link between epigenetic chromatin remodeling and plant immunity. Furthermore, I have established that the genome-wide deposition of H2A.Z significantly increases under biotic stress. Overall, since H2A.Z is highly conserved among eukaryotes, including humans, this information likely provides a framework to test the role of histone replacement in immunity in a wide range of eukaryotic systems.

CHAPTER V

Materials and Methods

Plant lines and growth condition

The following lines were obtained from TAIR (The Arabidopsis Information Resource): *act1* – SALK_093023, *arp4* – SAIL_760_H04, *swc2* – SALK_091595, *swc5* – SALK_201865, *swc6* – SAIL_1142, *pie1* – SALK_013922, *rvb1-7* – SALK_117490, *rvb1-8* – SALK_133101, *yaf9* – SALK_9041175. *suf3* [54] was obtained from Dr. Ilha Lee. BLRP-H2A.Z and *h2a.z* [29] was obtained from Dr. Daniel Zilberman. Plants were grown in soil in a growth chamber under long-day photoperiod (16 hours light) at 23°C and 60% relative humidity. Wild-type and all mutant lines are from Col-0 ecotype, except that swc6 is in the Col-3 ecotype.

DNA constructs and molecular biology techniques

Clones amplified via PCR were cloned into pJET (Thermo Fisher). All Y2H constructs consisted of the coding sequence of the gene cloned into either pP6 (Gal4 AD) or pB27 (LexA BD) in the yeast strain L40 or Y187, respectively. All Co-IP constructs consisted of the coding sequence of the gene cloned into the pER vector which was tagged at the 3' end with triple FLAG (pET-FLAG) or sextuple Myc (pET-Myc) tags. DNA extraction, ligation, digestion, miniprep, band isolation, gel purification, transformations, and cDNA synthesis were all performed as described [64].

Yeast Two-Hybrid

Yeast two-hybrid was performed as described in a manufacturer manual (Clontech). Genes tested in pP6 or pB27 plasmids were transformed into L40 and Y187 yeast strains, respectively. One colony from each construct was stored in glycerol stock and used for each trial. The stocks were streaked onto plates containing complete media lacking uracil and leucine (-UL in the case of pP6 constructs) and onto those lacking uracil and tryptophan (-UW in the case of pB27 constructs). After 3 days, the yeast was inoculated into 1 mL of the corresponding –UL and –UW media to grow at 28°C for 8 hours. YPD media (160 µl) was then added to sterile tubes along with 20 µL of each yeast solution of the set to be tested. After mixing, the tubes were set to shake at 250 rpm for 16 hours at 28°C to allow for mating of the yeast. Samples were then spun down at 14,000 rpm for 20 seconds and the supernatant was removed to wash the yeast with 1 mL of water. Tubes were then spun down a second time at 14,000 rpm for 20 seconds and 800 µL of water were removed. The remaining solution was mixed and 5 µL were plated onto positive control (-UMWL) plates and experimental (-UMWLH) plates as well as experimental plates that contained 0.1 mM 3 amino-1,2,4-triazole to test for the strength of interactions.

Transient Gene Expression in *N. benthamiana*

Transient gene expression in *N. benthamiana* was performed as described [65]. Chromatin remodeling factors were cloned into the pER8-FLAG vector and then

transformed into Agrobacterium strain GV2260. Once obtained in glycerol stock, solutions were then, along with Myc-MORC1 and pBA-TEV, streaked onto LB plates containing the antibiotic spectinomycin for two days at 28°C. pBA-TEV was used to enhance transient expression by suppressing gene silencing [13]. pBIN-GFP was grown on plates containing kanamycin. Samples were then inoculated in their corresponding liquid media for one day at 28°C. After 24 hours, 1/100 of the solution was inoculated in LB containing 10 mM MES at pH 5.7 and incubated at 28°C. After another 24 hours, samples were spun down at 25,000xg for 5 minutes at 20°C and washed three times with 1 ml of 10 mM MES at pH 5.7. After the third washing and centrifugation, samples were resuspended in 1 ml 10mM MES at pH 5.7 containing 10 mM acetosyringone. The OD was adjusted to 0.5 and the samples were incubated at room temperature, shaking at 250 rpm. After 2-3 hours, solutions were mixed with a 1:1:1 ratio of solution containing the chromatin remodeling factor-FLAG (or GFP-FLAG), Myc-MORC1, as well as pBA-TEV. The mixed solutions were then infiltrated into leaves of *Nicotiana benthamiana* using an older leaf from one plant and a younger leaf from another. After one day, 30 μM estradiol in 0.1% Tween-20 was sprayed on the leaves to induce expression of constructs and plants were transferred to a low-light setting. Tissue was then collected after two days.

Co-immunoprecipitation

Co-immunoprecipitation (Co-IP) was performed as described [66]. Infiltrated leaves were ground to a liquid using 750 μl of extraction buffer while Sephadex columns (GE Healthcare) were washed three times with 1 ml immunoprecipitation (IP) buffer. Samples were then collected and spun at 5,000xg at 4°C for 5 minutes. Each supernatant (500 μl) was pipetted into a separate column, followed by 1 ml of IP buffer. While the sample was running through the column, anti-mouse IgG agarose beads (Sigma; ~20 μl per sample) were washed three times with 1 ml IP buffer spun at 5,000xg at 4°C for 10 seconds and finally mixed with 1 ml IP buffer. Once the samples had run through the columns, the flow-through was collected and a designated amount of beads were allotted to each sample (1000 μl/number of samples x 0.9). The samples were then rotated in 4°C for 2 hours. The beads carrying the target antibody conjugated with agarose (~20 μl per sample) were washed three times with 1 ml IP buffer spun at 5,000xg at 4°C for 10 seconds and finally mixed with 1 ml IP buffer. New tubes were labeled for input and immunoprecipitated (IP) extracts. Samples were then spun at 5,000xg at 4°C for 5 minutes. Upon centrifugation, 950 μl of supernatant were transferred to IP tubes containing target antibody beads (1000 μl/number of samples x 0.9) and 45 μl were aliquoted to input tubes containing 15 μl of 4x SDS sample buffer containing DDT at 66 mg/ml. The input tubes were stored in -80°C and the IP tubes were set to rotate for 8 hours or more in 4°C. Tubes were then washed three times with 1 ml IP buffer at 5,000xg at 4°C for 10 seconds with a final addition of 1 ml IP buffer. These tubes were then rotated for 30 minutes at 4°C, washed three times, rotated again at 4°C for 30 minutes, and again washed three times. Tubes were then transferred to room temperature and rotated for 10 minutes upon which they were spun down at 5,000xg for 10 seconds. Supernatant was removed and 4x SDS sample buffer containing DTT at 60 mg/ml was added (30 μl per tube) before proceeding with the immunoblot.

Immunoblot

Immunoblot analysis was performed as described [67]. Frozen tissue samples were ground with beads and mixed with 4x SDS sample buffer containing DTT at 60 mg/ml. Once homogenized, they were then boiled for 5 minutes and centrifuged at 21,100xg for 2 minutes. Supernatant was loaded (5 µl per sample) into polyacrylamide gels, along with 5 µl of protein ladder (Bio-Rad). Each gel was then transferred onto a PVDF membrane (Immobilon) using 10x Transfer Buffer. Membranes were soaked in methanol and allowed to dry for 15 minutes after which they were again soaked in methanol and subsequently washed with PBS Buffer three times within 5 minutes. Membranes were then left overnight shaking at 200rpm at 4°C in 3B1M Buffer with the designated antibody. After incubation, membranes were washed with PBS, PBS-T, and PBS Buffer twice each for 5 minutes for a total washing of 30 minutes. Membranes were then covered in ECL2 solution and imaged using a EM-CCD camera (Hamamatsu). Antibodies used include HRP-conjugated anti-Myc (Santa Cruz Biotechnology; 1:10,000), HRP-conjugated anti-FLAG (Sigma; 1:20,000), anti-PEPC [Rockland; 1:10,000, secondary antibody: HRP-conjugated anti-Rabbit (Abcam; 1:10,000)], anti-Histone H3 [(Abcam; 1:10,000, secondary antibody: HRP-conjugated anti-Rabbit (Abcam; 1:10,000)], HRP-conjugated streptavidin (Thermo Fisher; 1:2,000).

Resistance Assay

Bacterial resistance assay using an EM-CCD camera was performed as follows: Plants were syringe infiltrated with 10^5 cfu/ml *Pseudomonas syringae* pv. *tomato DC3000* or $5x10^5$ cfu/ml *Pseudomonas syringae* pv. *tomato DC3000 (avrRpt2)* in 10mM $MgCl_2$. Images were taken 2 days post infiltration using a high throughput EM-CCD camera. Using the HCImageLive software, the quantitative value of luminescence from each leaf was obtained based on the intensity.

Bacterial resistance assay using a conventional plating method was performed as follows: Plants were syringe infiltrated with 10^5 cfu/ml *Pseudomonas syringae* pv. *maculicola* in 10mM $MgCl_2$. Three leaf disks were obtained of each plant from the same line using a 0.5 cm diameter borer and homogenized in a shaker for 2 minutes using a bead and 300 µl of 0.01% Triton X-100. Samples were vortexed briefly and centrifuged at 300xg for 30 seconds. The upper 200 µl was obtained and serially diluted. 20 µl of all dilutions were then plated on LB kanamycin plates and colonies were counted after 24 hours.

Generation of transgenic lines

Transformation of Arabidopsis was performed as described [12]: genes tested were cloned into the Agrobacterium strain MP90, which was inoculated in 1 ml LB + antibiotic overnight. After incubation, tubes were spun down at 4,700xg for 20 minutes and the OD was adjusted to 0.5 using Infiltration Buffer for a total volume of 200 ml. 5-6 week old Col-0 and *morc1 morc2* were used for dipping. Plants were placed upside down so that inflorescences were completely submerged in the Infiltration Buffer and subjected to a vacuum for 5 minutes. Plants were then placed horizontally in the dark for two days and then exposed to 16-hour light conditions until the inflorescences gravitated toward the light, after which the plants were then placed upright under the light for the duration

of their life cycle. Seeds were then collected from mature plants and plated onto ½ MS + Hygromycin plates for selection. Selected plants were transferred onto soil and grown in 16-hour light condition. 2 week-old leaves from each T_1 plant were submerged in 30 μM estradiol for 2 days and then subjected to western blot.

Subcellular Fractionation

Subcellular fractionation was performed as described [68]: two grams of leaf tissue was collected and submerged in precooled diethyl ether for three minutes, followed by washing three times with deionized water. Tissue was homogenized using a mechanical homogenizer in 13ml NHB (Nucleus Homogenization Buffer; 25mM PIPES, 10mM NaCl, 5mM EDTA, 250mM Sucrose, 0.15mM Spermine, 0.5mM Spemidine, 5mM DTT (dithiothreitol), 0.5% TritonX-100, 1X Plant protease inhibitor cocktail). The samples were stored on ice for five minutes then filtered through double-layered Miracloth (Millipore) Samples were then centrifuged at 1,000xg for five minutes at 4°C. The supernatant was saved for further "nucleus-depleted" fraction (10 ml) and the rest of the supernatant was removed by vacuum. The pellet was washed with NHB (1 ml) using a pre-cut pipet tip. The solution was transferred to a new 1.5 ml Eppendorf tube and centrifuged at 1,000xg for one minute at 4°C and the supernatant was removed. This washing was repeated two or three times to remove chloroplast contamination. The pellet was then resuspended in 1 ml NIB (Nuclear Isolation Buffer; 1M Sucrose, 10mM Tris-HCl (pH 7.2), 5mM MgCl2, 10mM β-mercaptoethanol). Nuclear extract was further purified using Percoll density gradient centrifugation. In a 5 ml tube, 1 ml each, 80% and 35% percoll in NIB and nuclear extract were layered from bottom to top respectively and centrifuged at 635xg for 5 minutes followed by 10154xg for 15 minutes at 4°C. The enriched nuclei layer at the intersection of 35% and 80% percoll was isolated, mixed with 5 ml NIB, and pelleted by spinning at 4000xg at 4°C and used for further experimentation. The nucleus pellet was resuspended in 25 μl of 4x SDS sample buffer containing 60 mg/ml DTT. From the 10 ml of saved "nucleus-depleted" fraction, 1 ml was added to two ultra-centrifuge tubes each and centrifuged at 100,000xg for one hour at 4°C. The microsomal pellet was resuspended in 25 μl of 4x SDS sample buffer containing 60 mg/ml DTT. The supernatant was then transferred to a column and centrifuged at 4,000xg for 30 minutes at 4°C. The flow-through was discarded and the concentrated cytosolic solution remaining in the filter column was transferred to a 1.5 ml Eppedorf tube with 40 μl of 4x SDS sample buffer containing 60 mg/ml DTT.

Modified Co-IP procedure for subcellular fractions

The nucleus and microsome pellets were resuspended in enough IP buffer to total 500 μl. The concentrated cytosolic solution was resuspended in enough IP buffer to total 1 ml. The nucleus and microsome fractions were then sonicated for 20 minutes, with alternating 5 minutes of pulse on and off time. These fractions were then subject to Co-IP procedure described earlier.

RNA preparation and its quantitation analysis

Two leaves of Col-0 and the *h2a.z* mutant were infiltrated with 10 mM $MgCl_2$ (mock) or 10^6 cfu/ml virulent *Pst.* Two infiltrated leaves of different plants were collected in a single tube at 6, 24, 48, and 72 hours as well as non-treated (naïve) tissue. RNA was

extracted using the Trizol reagent (Invitrogen), converted to cDNA by SuperScript RT (Invitrogen), and subjected to qRT-PCR. Thermo Scientific, Maxima SYBR Green qPCR Master Mix (2X) was used for qRT-PCR. Thermal profile used for qRT-PCR was: UDG (uracil-DNA glycosylase) incubation at 50 °C for 2min., polymerase activation at 95 °C for 10min., 40 PCR cycles of 95 °C for 25 sec and 60 °C for 1min followed by melt curve cycle at 95, 55 and 95 °C respectively for 15 seconds each.

Chromatin immunoprecipitation quantitative polymerase chain reaction (ChIP-qPCR)

ChIP was performed largely as described in [69].

2 grams of leaf tissue was obtained in a 25 ml centrifuge tube and mixed well in 35 ml cross-linking buffer. A sponge was added on top of the leaves and submerged, then cross-linking buffer was added to a total of 40 ml. Each tube was then subjected to a vacuum for 1 hour with the lid removed, and the vacuum was released slowly for the last 10 minutes. 1 M glycine was then added (1/10 of the total volume in tubes) and mixed well. Samples were then vacuumed for 3 minutes with a slow release of 2 additional minutes. The buffer and glycine were then decanted and the leaves were rinsed with double-deionized water three times and excess water was removed using a paper towel. Leaves were then submerged in 13 ml cold NHB buffer homogenized for 55 seconds, and kept in ice for 5 minutes. The solution was then filtered using double-layered Miracloth (Millipore), and then centrifuged at 1,000xg for 5 minutes at 4°C. The supernatant was removed and the pellet was resuspended in 1 ml NHB buffer using a pre-cut pipet tip. The solution was then transferred to an Eppendorf tube and centrifuged again at 1,000xg for 1 minute at 4°C. The wash was repeated until the supernatant was clear. The pellet was then resuspended in 280 µl of IP buffer (+ 1% SDS, 1% NP-40) and 300 µl were transferred to 2 ml flat cap tubes to be sonicated, and 10 µl were saved to check the efficiency of the sonication. Samples were then sonicated for 20 minutes, with alternating 5 minutes of pulse on and off time. Next, samples were centrifuged at full speed (21,100xg) for 10 minutes at 4°C and the supernatant (260 µl) was transferred to a new 2 ml flat cap tube and diluted up to 1.8 ml with IP buffer (+ 1% SDS, 1% NP-40), 10-20 µl were transferred to a tube for checking sonication efficiency, while the tube containing the pellet was tossed. Agarose salmon sperm beads were added (25 µl per sample) to a new tube and washed with 500 ml IP buffer (+ 1% SDS, 1% NP-40) three times, each time undergoing a quick spin. The beads were resuspended in enough buffer for each sample to obtain 25 µl of beads for preclearing. The tubes were then rotated for at least 1 hour at room temperature, after which the tubes were centrifuged and 1.7 ml of supernatant were transferred to a new Eppendorf tube to undergo ChIP, while 130 µl were transferred to a new Eppendorf tube as the Input sample. The tubes with the leftover preclearing beads were tossed. Streptavidin-conjugated magnetic beads (Thermo Fisher) were then added (50 µl per sample) to a new Eppendorf tube and washed three times with 500 ml IP buffer (+ 1% SDS, 1% NP-40). Beads were then resuspended in enough IP buffer (+ 1% SDS, 1% NP-40) for each sample to receive 50 µl of beads and tubes were rotated overnight at room temperature. Samples were then placed on a magnetic tube holder and the supernatant was transferred to a tube as the depleted fraction optionally, for western blotting. The remaining beads were then resuspended in 1 ml IP buffer (+ 1% SDS) and rotated for 15 minutes (this step was repeated). The supernatant was removed

and the beads were washed with 1 ml LiCl wash buffer and tubes rotated for 5 minutes. The beads were then washed with 1 ml TE buffer and tubes rotated for 5 minutes (this step was repeated). 250 µl of elution buffer (+ 1% SDS) was added to the beads and tubes were rotated for 15 minutes. Tubes were placed on a magnetic tube holder and after 2 minutes the supernatant was transferred to a new Eppendorf tube for the eluted sample. 280 µl of elution buffer (+ 1% SDS) was added to the beads and tubes were rotated for 15 minutes and the supernatant was added to the tube of the eluted sample. 30 µl of the eluted sample was transferred to a new tube for running an optional western blot. Another round of elution was performed in which 530 µl of elution buffer (+ 2% SDS) was added to the beads and tubes were boiled for 3 minutes. 30 µl of this solution was transferred to a new Eppendorf tube as the second eluted sample collection for western blot. The second eluted sample containing 500 µl was then subjected to reverse-crosslinking in which 20 µl of 5 M NaCl was added to the tube. 100 µl of the 130 µl saved input was diluted with elution buffer (+ 2% SDS) up to 500 µl and 20 µl of 5 M NaCl was added to the tube. Tubes were then subjected to 65°C for at least 6 hours for reverse-crosslinking. Samples were then mixed with 10 µl of 0.5M EDTA, 20 µl 1M Tris-Cl pH 6.5, a 2 µl of 20 mg/ml proteinase K per tube and incubated for 1 hour at 45°C. DNA was then purified according to QIAquick PCR purification kit, and the procedure was followed per the manufacturer's recommendation. Immunoprecipitated DNA was diluted and used for qPCR. DNA purified from input chromatin was used as reference to calculate fold enrichment. Thermo Scientific, Maxima SYBR Green qPCR Master Mix (2X) was used for qPCR. Thermal profile used for qPCR was: UDG (uracil-DNA glycosylase) incubation at 50 °C for 2min., polymerase activation at 95 °C for 10min., 40 PCR cycles of 95 °C for 25 sec and 60 °C for 1min followed by melt curve cycle at 95, 55 and 95 °C respectively for 15 seconds each.

Oligonucleotides used in cloning, RT-PCR and ChIP-qPCR

Oligonucleotides used in this study are listed in Table 3.

Table 3. List of oligonucleotides used in cloning, genotyping, RT-PCR, and ChIP-qPCR.

Primer name	Sequence
3' AD seq-pGAD seq	AGATGGTGCACGATGCACAG
3' DNA-BD-pGBK seq	TTTTCGTTTTAAAACCTAAGAGTC
pER8 F_NEW	AATATGCTCGACTCTAGGATCTTC
3A-ter	TGATACGGACGAAAGCTGG
PIE1 F BamH1	GGATCCATATGGCGTCTAAAGGTGGTAAATCT
PIE1 R BamH1	GGATCCCTACTCTATTTCTGAGATATCCG
Tip41-Like-R-q	GGATACCCTTTCGCAGATAGAGAC
Tip41-Like-F-q	GCGATTTTGGCTGAGAGTTGAT
act1 SALK 093023c LP	TTTGGATCTGGGTGTCTTGAG
act1 SALK 093023c RP	GTGAAAGAGTAACCACGCTCG
arp4 SAIL 760 H04 LP	ATAGACCGCCTCAAAGGTAGC
arp4 SAIL 760 H04 RP	AGACTTACGGAAGGGAAAACG
swc2 SALK 091595 LP	CACGGCAAATGGATCATAAAG
swc2 SALK 091595 RP	TTAACTGCGGAGTTTTGATGG
swc5 SALK 201865c LP	TTTTGGCAGAAAATTTATTTTGG
swc5 SALK 201865c RP	GCCAAACACAAACTCAAACAAG
swc6 SAIL 1142 CO3 LP	AGCACATAAAAACAGCCATGG
swc6 SAIL 1142 CO3 RP	AAGTTGTTAAAGGCCCAATGG
pie1 SALK 013922 LP	CACCGCTTGATGAGTCTCTTC
pie1 SALK 013922 RP	GAGAGAAAGAAACCCGAGCTC
rvb1 SALK 117490c _LP	TTTGCAGAGGGACTGATATGC
rvb1 SALK 117490c RP	TCTGTTCCCAACCGTGATAAG
rvb1 SALK 133101 LP	TAGATGAAGGTGTGGCAGAGC
rvb1 SALK 133101 RP	AAGTTTGAATCTCACGACCATG
yaf9 SALK 041175c LP	GGACCTTTTCGTCGGATTTAG
yaf9 SALK 041175c RP	ATTCTCACCAAAAACGTTCCC
LBb-1 SALK	GCGTGGACCGCTTGCTGCAACT
LB2 SAIL	GCTTCCTATTATATCTTCCCAAATTACCAATACA
PIE1-F2-1866	GCGGAAACTCAAGAGACAAGGAT
PIE1-R1-2123	TGCATAAGTGACCACAGTTCCAT
PIE1-F3-4540	GCCAAATATAAATCCCTGAAGAA
PIE1-R2-4270	AATCTCTTTTCTTGCCCTTCATA
SWC2-SacII R	CCGCGGTTAATCTGAATCTTCTTCACTCTC
SWC2-SacII F	CCGCGGCCATGGAAATCGATGAAGAAGAGCCA
Act1 -F-Asc1	GGCGCGCCATGGCTGATGGTGAAGACA
Act1 -R-Asc1	GGCGCGCCGAAGCACTTCCTGTGAACAA
Arp4 -F-Asc1	GGCGCGCCATGTACGGCGGAGATGAAGTGTC
Arp4 -R-Asc1	GGCGCGCCAGGGCATTTTCTCTGAATGT
Swc2-F-Asc1	GGCGCGCCATGGAAATCGATGAAGAAGAGC
Swc2-R-Asc1	GGCGCGCCATCTGAATCTTCTTCACTCT
Swc5-F-Asc1	GGCGCGCCATGGATCTCATGAGCAATCGC
Swc5-R-Asc1	GGCGCGCCTACATCATCGTGTCTTCTCT
Swc6-F-Asc1	GGCGCGCCATGGAGGAAGAGATGTCGAACCG
Swc6-R-Asc1	GGCGCGCCTGCAACAAATTTCTGACAAC

Table 3, Continued. List of oligonucleotides used in cloning, genotyping, RT-PCR, and ChIP-qPCR.

Suf3-F-Asc1	GGCGCGCCATGTCAAACATCGTTGTTCTAG
Suf3-R-Asc1	GGCGCGCCATGAAAGAATCGTCTACGAC
Pie1-F-Asc1	GGCGCGCCATGGCGTCTAAAGGTGGTAAATC
Pie1-R-Asc1	GGCGCGCCTCTATTTCTGAGATATCCG
Rvb1-F-Asc1	GGCGCGCCATGGAGAAAGTAAAGATTGAAGA
Rvb1-R-Asc1	GGCGCGCCTGAGATGTATTTTTCTTGTT
Yaf9-F-Asc1	GGCGCGCCATGACGAACAGCTCGTCATC
Yaf9-R-Asc1	GGCGCGCCCAGGTCTGATCCTGTTTTAA
RIN1 F-1	GGCCGGACGGGCCATGGAGAAAGTAAAGATTGAAGAA
RIN1 R-126	GGCCCCAGTGGCCTTAACGTAGACCAATGGCACGTCTAAA
RIN1 F-127	GGCCGGACGGGCCATCAAGGAAACCAAAGAAGTCTAT
RIN1 R-300	GGCCCCAGTGGCCTTATCCTGGAACAAGCTCTGCCACACC
RIN1 F-301	GGCCGGACGGGCCGTTCTATTTATTGATGAGGTTCAT
RIN1 R-458	GGCCCCAGTGGCCTCATGAGATGTATTTTTCTTGTTG
RIN1-5 F primer	GGCGCGCCATGATCAAGGAAACCAAAGAAGTCTAT
RIN1-5 R primer	GGCGCGCCTCCTGGAACAAGCTCTGCCACACC
HTA8-F (RP)	TCCAGAGAGGATGATGATGAAACTGAA
HTA8-R (LP)	TCCAGATCCGTCGTCGAAATCA
FLAG-TDNA-LB1	CGTGTGCCAGGTGCCCACGGAATAGT
HTA11-F (RP)	TTGTTTGACTGTGTACGGTTAGATCTAGA
HTA11-R (HTA11 in TKO LP)	CAGAACATTGCACATACTAGAACCAAACA
SALK-TDNA-LB1	TGGTTCACGTAGTGGGCCATCG
HTA9-F (LP)	TAACACAAAGTACGCTGATCGAACGAACA
HTA9-R (HTA9 in TKO RP)	GATCGCGTTTAAGTGGTAGATCGATGAGA
SALK-TDNA-LB1	TGGTTCACGTAGTGGGCCATCG
HTA11-R (LP)	ATGTCCAGAAGAGGTCAACACTAG
HTA9-R (RP)	GAAGAAGCCTATCACTCGTTCTTC
HTA8-RT-F	GCTGGTAAAGGTGGGAAAGGGCTTCTAGC
HTA8-RT-R	TCAGCAGTCAAGTATTCTAGAATTGATGAAGCGTAAACAG
HTA11-RT-F	TCGTTCCCTTGATGAGTGTGTCCAGC
HTA11-RT-R	GACTCGTAGCTGCGAAGACGATGGCTGC
HTA9-RT-F	ACCCAGCGGTAGCGACAAGGATAAGGAC
HTA9-RT-R	TTGTGCGATCTCCTTTCTCTTTCAATCTC
HTA9-Q-F	AGCGGTAGCGACAAGGATAAG
HTA9-Q-R	TGGTAGGGTGCATCGTCTGT
RVB1_qRT_F	GAAGAATTAACCGTGGATGAAGA
RVB1 qRT R	ATATCAGCCTTGCAAATATTGTC
RVB1-F (qPCR)	GGGAAGCAAGGTTCCATTCTGTCC
RVB1-R (qPCR)	GACAGCTCGGTGACCTCCCCTTCA
PIE1-F (qPCR)	GGCCAAACTGAGAGGTACTCAACC
PIE1-R (qPCR)	AGACCTGCAGAAGAATTTATCTCT
Sal1-MORC1 F	GTCGACATGGCGAAAAATTACACAGTCGCCGA
MORC1-Apa1 R_new	GGGCCCAACTTGTTGCATCTCCTTCTTCTT

Table 3, Continued. List of oligonucleotides used in cloning, genotyping, RT-PCR, and ChIP-qPCR.

Sal1-SUF3 F	GTCGACATGTCAAACATCGTTGTTCTAGAC
SUF3-Apa1 R new	GGGCCCATGAAAGAATCGTCTACGACAC
Sal1-RVB1 F	GTCGACATGGAGAAAGTAAAGATTGAAGAAA
RVB1-Apa1 R new2	GGGCCCTGAGATGTATTTTTCTTGTTGC
PR1-R QRT	CCACCATTGTTACACCTCACTTT
PR1-F QRT	AAAACTTAGCCTGGGGTAGCGG
PR2-R QRT	TGTAAAGAGCCACAACGTCC
PR2-F QRT	ATCAAGGAGCTTAGCCTCAC
PR2 SMQ QT R	AAAATCACAAGCTTAGGGTAGAAA
PR2 QT F	AACACAAATCATGCATCTAACCAG
PR5-R QRT	GAAGCACCTGGAGTCAATTC
PR5-F QRT	CTCTTCCTCGTGTTCATCAC
PR5-F q New	CGGCATTGCTGTTATGGC
PR5-R q New	CTGTCGGGAAGCACCTGGAG
UBC9-R-q	ACTCGTACTTGTTCTTGTCTGTCTTGT
UBC9-F-q	ACAATTTCCAAGGTGCTGCTATC
Act-R-q	CCCCAGCTTTTTAAGCCTTT
Act-F-q	AGTGTCTGGATCGGTGGTTC
Tip41-Like-R-q	GGATACCCTTTCGCAGATAGAGAC
Tip41-Like-F-q	GCGATTTTGGCTGAGAGTTGAT
Tip41-cDNA-1F	CCGGCGATTCAGATGGAGAC
Tip41-cDNA-1R	CGACAGCGAGAGAAGTGAGAATC
BirA-F2	TGCGTGACTGGGGCGTTGAT
BirA-R2	CGCCGGGCCTTGTTCCA

REFERENCES

1. Tameling, W.I.L. and F.L.W. Takken, *Resistance proteins: scouts of the plant innate immune system.* European Journal of Plant Pathology, 2007. **121**(3): p. 243-255.

2. Felix, G., *Plants have a sensitive perception system for the most conserved domain of bacterial flagellin.* The Plant Journal, 1999. **18**(3): p. 265-276.

3. Zipfel, C., *Bacterial disease resistance in Arabidopsis through flagellin perception.* Nature, 2004. **428**: p. 764-767.

4. Zipfel, C. and G. Felix, *Plants and animals: a different taste for microbes?* Curr Opin Plant Biol, 2005. **8**(4): p. 353-60.

5. Nurnberger, T. and B. Kemmerling, *Receptor protein kinases--pattern recognition receptors in plant immunity.* Trends Plant Sci, 2006. **11**(11): p. 519-22.

6. Roudier, F., et al., *Integrative epigenomic mapping defines four main chromatin states in Arabidopsis.* EMBO J, 2011. **30**(10): p. 1928-38.

7. Jones, J.D. and J.L. Dangl, *The plant immune system.* Nature, 2006. **444**(7117): p. 323-9.

8. Chisholm, S.T., et al., *Host-microbe interactions: shaping the evolution of the plant immune response.* Cell, 2006. **124**(4): p. 803-14.

9. Birch, P.R., et al., *Trafficking arms: oomycete effectors enter host plant cells.* Trends Microbiol, 2006. **14**(1): p. 8-11.

10. Catanzariti, A.M., P.N. Dodds, and J.G. Ellis, *Avirulence proteins from haustoria-forming pathogens.* FEMS Microbiol Lett, 2007. **269**(2): p. 181-8.

11. Grant, S.R., et al., *Subterfuge and manipulation: type III effector proteins of phytopathogenic bacteria.* Annu Rev Microbiol, 2006. **60**: p. 425-49.

12. Bechtold, N., J. Ellis, and G. Pelletier, *In planta Agrobacterium mediated gene transfer by infiltration of adult Arabidopsis thaliana plants.* Comptes Rendus de l'Academie des Sciences, Serie III. Sciences de la Vie/Life Sciences, 1993. **316**(10): p. 1194-1199.

13. Kang, H.G., et al., *CRT1, an Arabidopsis ATPase that interacts with diverse resistance proteins and modulates disease resistance to turnip crinkle virus.* Cell Host Microbe, 2008. **3**(1): p. 48-57.

14. Kang, H.G., et al., *CRT1 is a nuclear-translocated MORC endonuclease that participates in multiple levels of plant immunity.* Nat Commun, 2012. **3**: p. 1297.

15. Kang, H.G., et al., *Endosome-associated CRT1 functions early in resistance gene-mediated defense signaling in Arabidopsis and tobacco.* Plant Cell, 2010. **22**(3): p. 918-36.

16. Moissiard, G., *MORC Family ATPases Required for Heterochromatin Condensation and Gene Silencing.* Science, 2012. **336**(6087): p. 1448-1451.

17. Matzke, M., A. and Rebecca A. Mosher, *RNA-directed DNA methylation: an epigenetic pathway of increasing complexity.* Nature Reviews Genetics, 2014. **15**: p. 394-408.

18. Doerks, T., et al., *Systematic identification of novel protein domain families associated with nuclear functions.* Genome Res, 2002. **12**(1): p. 47-56.

19. Clapier, C.R. and B.R. Cairns, *The biology of chromatin remodeling complexes.* Annu Rev Biochem, 2009. **78**: p. 273-304.

20. Berr, A., S. Shafiq, and W.H. Shen, *Histone modifications in transcriptional activation during plant development.* Biochim Biophys Acta, 2011. **1809**(10): p. 567-76.

21. Kobor, M.S., et al., *A protein complex containing the conserved Swi2/Snf2-related ATPase Swr1p deposits histone variant H2A.Z into euchromatin.* PLoS Biol, 2004. **2**(5): p. E131.

22. Krogan, N.J., *A Snf2 Family ATPase Complex Required for Recruitment of the Histone H2A Variant Htz1.* Molecular Cell, 2003. **12**(6): p. 1565-1576.

23. March-Diaz, R., et al., *SEF, a new protein required for flowering repression in Arabidopsis, interacts with PIE1 and ARP6.* Plant Physiol, 2007. **143**(2): p. 893-901.

24. Hartley, P.D. and H.D. Madhani, *Mechanisms that specify promoter nucleosome location and identity.* Cell, 2009. **137**(3): p. 445-58.

25. Wan, Y., et al., *Role of the histone variant H2A.Z/Htz1p in TBP recruitment, chromatin dynamics, and regulated expression of oleate-responsive genes.* Mol Cell Biol, 2009. **29**(9): p. 2346-58.

26. Venters, B.J. and B.F. Pugh, *A canonical promoter organization of the transcription machinery and its regulators in the Saccharomyces genome.* Genome Res, 2009. **19**(3): p. 360-71.

27. March-Diaz, R. and J.C. Reyes, *The beauty of being a variant: H2A.Z and the SWR1 complex in plants.* Mol Plant, 2009. **2**(4): p. 565-77.

28. Alvarez, M.E., F. Nota, and D.A. Cambiagno, *Epigenetic control of plant immunity.* Mol Plant Pathol, 2010. **11**(4): p. 563-76.

29. Zilberman, D., *Histone H2A.Z and DNA methylation are mutually antagonistic chromatin marks.* Nature, 2008. **456**: p. 125-129.

30. Coleman-Derr, D. and D. Zilberman, *Deposition of histone variant H2A.Z within gene bodies regulates responsive genes.* PLoS Genet, 2012. **8**(10): p. e1002988.

31. Dhillon, N., et al., *H2A.Z functions to regulate progression through the cell cycle.* Mol Cell Biol, 2006. **26**(2): p. 489-501.

32. Smith, A.P., et al., *Histone H2A.Z regulates the expression of several classes of phosphate starvation response genes but not as a transcriptional activator.* Plant Physiol, 2010. **152**(1): p. 217-25.

33. Kumar, S.V. and P.A. Wigge, *H2A.Z-containing nucleosomes mediate the thermosensory response in Arabidopsis.* Cell, 2010. **140**(1): p. 136-47.

34. Morrison, A.a.X.S., *Chromatin remodelling beyond transcription: the INO80 and SWR1 complexes.* Nature Reviews Molecular Cell Biology, 2009. **10**: p. 373-384.

35. Papamichos-Chronakis, M., et al., *Global regulation of H2A.Z localization by the INO80 chromatin-remodeling enzyme is essential for genome integrity.* Cell, 2011. **144**(2): p. 200-13.

36. Nguyen, V.Q., et al., *Molecular architecture of the ATP-dependent chromatin-remodeling complex SWR1.* Cell, 2013. **154**(6): p. 1220-31.

37. March-Diaz, R., et al., *Histone H2A.Z and homologues of components of the SWR1 complex are required to control immunity in Arabidopsis.* Plant J, 2008. **53**(3): p. 475-87.

38. Holt III, B.F., *An Evolutionarily Conserved Mediator or Plant Disease Resistance Gene Function Is Required for Normal Arabidopsis Development.* Developmental Cell, 2002. **2**(6): p. 807-817.

39. Gribun, A., et al., *Yeast Rvb1 and Rvb2 are ATP-dependent DNA helicases that form a heterohexameric complex.* J Mol Biol, 2008. **376**(5): p. 1320-33.

40. Ducat, D., et al., *Regulation of microtubule assembly and organization in mitosis by the AAA+ ATPase Pontin.* Mol Biol Cell, 2008. **19**(7): p. 3097-110.

41. Fukada, Y., et al., *Gene expression analysis of the Murine model of amyotrophic lateral sclerosis: studies of the Leu126delTT mutation in SOD1.* Brain Res., 2007. **1160**: p. 1-10.

42. Venteicher AS, e.a., *Identification of ATPases pontin and reptin as telomerase components essential for holoenzyme assembly.* Cell, 2008. **132**: p. 945-957.

43. Zilberman, D., et al., *Histone H2A.Z and DNA methylation are mutually antagonistic chromatin marks.* Nature, 2008. **456**(7218): p. 125-9.

44. Gregory G. Tall, M.A.B., Philip D. Stahl, Bruce F. Horazdovsky, *Ras-activated endocytosis is mediated by the Rab5 guanine nucleotide exchange activity of RIN1.* Developmental Cell, 2001. **1**(1): p. 73-82.

45. Choi, K., et al., *Arabidopsis homologs of components of the SWR1 complex regulate flowering and plant development.* Development, 2007. **134**(10): p. 1931-41.

46. Zuo, J., Qi-Wen Niu and Nam-Hia Chua, *An estrogen receptor-based transactivator XVE mediates highly inducible gene expression in transgenic plants.* The Plant Journal, 2000. **24**(2): p. 265-273.

47. Zhiyong Gao, E.-H.C., Timothy K. Eitas, and Jeffery L. Dangl, *Correction for Ho et al., Itch E3 ubiquitin ligase regulates large tumor suppressor 1 tumor-suppressor stability.* Proceedings of the National Academy of Sciences, 2011. **108**(21): p. 8914-8914.

48. Siegel, J.N., *Effect of 3-amino-1,2,3-triazole on metabolism in algae.* Plant Physiol, 1966. **41**: p. 670-672.

49. Causier, B., *Studying the interactome with the yeast two-hybrid system and mass spectrometry.* Mass Spectrom Rev, 2004. **23**(5): p. 350-67.

50. Golemis, E.A. and R. Brent, *Fused protein domains inhibit DNA binding by LexA.* Mol Cell Biol, 1992. **12**(7): p. 3006-14.

51. Gyuris, J.e.a., *Cdi1, a human G1 and S phase protein phosphatase that associates with Cdk2.* Cell, 1993. **75**: p. 791-803.

52. Wu, W.H., et al., *Swc2 is a widely conserved H2AZ-binding module essential for ATP-dependent histone exchange.* Nat Struct Mol Biol, 2005. **12**(12): p. 1064-71.

53. Caplan, J., M. Padmanabhan, and S.P. Dinesh-Kumar, *Plant NB-LRR Immune Receptors: From Recognition to Transcriptional Reprogramming.* Cell Host Microbe, 2008. **3**(3): p. 126-35.

54. Choi, K., et al., *The FRIGIDA complex activates transcription of FLC, a strong flowering repressor in Arabidopsis, by recruiting chromatin modification factors.* Plant Cell, 2011. **23**(1): p. 289-303.

55. Chae, E., et al., *Species-wide genetic incompatibility analysis identifies immune genes as hot spots of deleterious epistasis.* Cell, 2014. **159**(6): p. 1341-51.

56. Fan, J., C. Crooks, and C. Lamb, *High-throughput quantitative luminescence assay of the growth in planta of Pseudomonas syringae chromosomally tagged with Photorhabdus luminescens luxCDABE.* Plant J, 2008. **53**(2): p. 393-9.

57. Cheng, C., et al., *Plant immune response to pathogens differs with changing temperatures.* Nat Commun, 2013. **4**: p. 2530.

58. Kakutani, T., Jeffrey A. Jeddeloh, Susan K. Flowers, Kyoko Munakata, and Eric J. Richards, *Developmental abnormalities and epimutations associated with DNA hypomethylation mutations.* Proceedings of the National Academy of Sciences, 1996. **98**(13): p. 12406-12411.

59. Czechowski, T., et al., *Genome-wide identification and testing of superior reference genes for transcript normalization in Arabidopsis.* Plant Physiol, 2005. **139**(1): p. 5-17.

60. Brickner, D.G., et al., *H2A.Z-mediated localization of genes at the nuclear periphery confers epigenetic memory of previous transcriptional state.* PLoS Biol, 2007. **5**(4): p. e81.

61. Jaskiewicz, M., U. Conrath, and C. Peterhansel, *Chromatin modification acts as a memory for systemic acquired resistance in the plant stress response.* EMBO Rep, 2011. **12**(1): p. 50-5.

62. Wessler, S.R., *Plant retrotransposons: turned on by stress.* Current Biology, 1996. **6**(8): p. 959-961.

63. Grandbastien, M.-A., *Activation of plant retrotransponsons under stress conditions.* Trends in Plant Science, 1998. **3**(5): p. 181-187.

64. Sambrook, J.D.W.R., *Molecular Cloning: a laboratory manual*. Third ed. Vol. 1-3. 2001, New York: Cold Spring Harbor Laboratory Press.

65. Frank L. Menke, H.-G.K., Zhixiang Chen, Jeong Mee Park, Dhirendra Kumar, and Daniel F. Klessig, *Tobacco transcription factor WRKY1 is phosphorylated by the MAP kinase SIPK and mediates HR-like cell death in tobacco.* MPMI, 2005. **18**(10): p. 1027-1034.

66. Sacco, M.A., S. Mansoor, and P. Moffett, *A RanGAP protein physically interacts with the NB-LRR protein Rx, and is required for Rx-mediated viral resistance.* Plant J, 2007. **52**(1): p. 82-93.

67. Kang, H.G. and D.F. Klessig, *Salicylic acid-inducible Arabidopsis CK2-like activity phosphorylates TGA2.* Plant Mol Biol, 2005. **57**(4): p. 541-57.

68. Mang, H.G., et al., *Abscisic acid deficiency antagonizes high-temperature inhibition of disease resistance through enhancing nuclear accumulation of resistance proteins SNC1 and RPS4 in Arabidopsis.* Plant Cell, 2012. **24**(3): p. 1271-84.

69. Saleh, A., R. Alvarez-Venegas, and Z. Avramova, *An efficient chromatin immunoprecipitation (ChIP) protocol for studying histone modifications in Arabidopsis plants.* Nat Protoc, 2008. **3**(6): p. 1018-25.